Chiral Effective Field Theory Beyond the Power-Counting Regime

Jonathan Hall

11th of July, 2011

CSSM, University of Adelaide

Overview

- Introduction
- Effective field theory for nucleons
  - Loop integrals
  - Renormalization
- Intrinsic scale model: pseudodata analysis
- Intrinsic scale: mass of the nucleon
- Establishing a robust method: a test example
- The magnetic moment of the nucleon
- The electric charge radius of the nucleon
- Conclusion

Aims

- Chiral Perturbation Theory describes the low-energy region, but is limited to use over a very small range of quark masses. How can we overcome this?

- Lattice Quantum Chromodynamics (QCD) is difficult to evaluate at physical quark mass, large volumes and small lattice spacings. How large is 'large enough' for a box size? We want to be able to extrapolate current results to the physical point.

- Using more of the available lattice results often entails regularization scale-dependence in extrapolations. But the lattice results themselves provide guidance on the choice of scale.

- This will lead us to realizing the presence of an intrinsic energy scale, embedded in lattice QCD results.

Aims

- Chiral Perturbation Theory describes the low-energy region, but is limited to use over a very small range of quark masses. How can we overcome this?
- Lattice Quantum Chromodynamics (QCD) is difficult to evaluate at physical quark mass, large volumes and small lattice spacings. How large is 'large enough' for a box size? We want to be able to extrapolate current results to the physical point.
- Using more of the available lattice results often entails regularization scale-dependence in extrapolations. But the lattice results themselves provide guidance on the choice of scale.
- This will lead us to realizing the presence of an intrinsic energy scale, embedded in lattice QCD results.

Aims

- Chiral Perturbation Theory describes the low-energy region, but is limited to use over a very small range of quark masses. How can we overcome this?
- Lattice Quantum Chromodynamics (QCD) is difficult to evaluate at physical quark mass, large volumes and small lattice spacings. How large is 'large enough' for a box size? We want to be able to extrapolate current results to the physical point.
- Using more of the available lattice results often entails regularization scale-dependence in extrapolations. But the lattice results themselves provide guidance on the choice of scale.
- This will lead us to realizing the presence of an intrinsic energy scale, embedded in lattice QCD results.

Aims

- Chiral Perturbation Theory describes the low-energy region, but is limited to use over a very small range of quark masses. How can we overcome this?
- Lattice Quantum Chromodynamics (QCD) is difficult to evaluate at physical quark mass, large volumes and small lattice spacings. How large is 'large enough' for a box size? We want to be able to extrapolate current results to the physical point.
- Using more of the available lattice results often entails regularization scale-dependence in extrapolations. But the lattice results themselves provide guidance on the choice of scale.
- This will lead us to realizing the presence of an intrinsic energy scale, embedded in lattice QCD results.

Why use χEFT?

- Chiral Effective Field Theory (χEFT) complements lattice QCD.
- It assists in understanding the consequences of dynamical chiral symmetry breaking.
- It provides a scheme-independent approach for investigating the properties of hadrons.
- In particular, it can be used in conjunction with lattice QCD results to extrapolate:
  - to physical quark mass,
  - to infinite lattice volume and the continuum limit.

Why use χEFT?

- Chiral Effective Field Theory (χEFT) complements lattice QCD.
- It assists in understanding the consequences of dynamical chiral symmetry breaking.
- It provides a scheme-independent approach for investigating the properties of hadrons.
- In particular, it can be used in conjunction with lattice QCD results to extrapolate:
  - to physical quark mass,
  - to infinite lattice volume and the continuum limit.

Why use χEFT?

- Chiral Effective Field Theory (χEFT) complements lattice QCD.
- It assists in understanding the consequences of dynamical chiral symmetry breaking.
- It provides a scheme-independent approach for investigating the properties of hadrons.
- In particular, it can be used in conjunction with lattice QCD results to extrapolate:
  - to physical quark mass,
  - to infinite lattice volume and the continuum limit.

Why use χEFT?

- Chiral Effective Field Theory (χEFT) complements lattice QCD.
- It assists in understanding the consequences of dynamical chiral symmetry breaking.
- It provides a scheme-independent approach for investigating the properties of hadrons.
- In particular, it can be used in conjunction with lattice QCD results to extrapolate:
  - to physical quark mass,
  - to infinite lattice volume and the continuum limit.

Why use χEFT?

- Chiral Effective Field Theory (χEFT) complements lattice QCD.
- It assists in understanding the consequences of dynamical chiral symmetry breaking.
- It provides a scheme-independent approach for investigating the properties of hadrons.
- In particular, it can be used in conjunction with lattice QCD results to extrapolate:
  - to physical quark mass,
  - to infinite lattice volume and the continuum limit.

Why use χEFT?

- Chiral Effective Field Theory (χEFT) complements lattice QCD.
- It assists in understanding the consequences of dynamical chiral symmetry breaking.
- It provides a scheme-independent approach for investigating the properties of hadrons.
- In particular, it can be used in conjunction with lattice QCD results to extrapolate:
    - to physical quark mass,
    - to infinite lattice volume and the continuum limit.

Why use χEFT?

- Chiral Perturbation Theory (χPT) is a low-energy theory where gluons and quarks can be replaced by effective degrees of freedom.
- χPT provides a formal expansion in terms of low-energy quark masses and momenta.
- The expansion is convergent if the quark masses and momenta are small enough so that higher-order terms are negligible. This is called the Power-Counting Regime (PCR).
- Within the PCR, χPT is renormalization scale-independent, and can be used to connect lattice simulations to the real world.
- Outside the PCR, χPT is, in general, scale-dependent, and care must be taken.
- Note: Here, we use 'χPT' to mean a massless renormalization scheme is used, but 'χEFT' allows different kinds of scheme.

Why use χEFT?

- Chiral Perturbation Theory (χPT) is a low-energy theory where gluons and quarks can be replaced by effective degrees of freedom.
- χPT provides a formal expansion in terms of low-energy quark masses and momenta.
- The expansion is convergent if the quark masses and momenta are small enough so that higher-order terms are negligible. This is called the Power-Counting Regime (PCR).
- Within the PCR, χPT is renormalization scale-independent, and can be used to connect lattice simulations to the real world.
- Outside the PCR, χPT is, in general, scale-dependent, and care must be taken.
- Note: Here, we use 'χPT' to mean a massless renormalization scheme is used, but 'χEFT' allows different kinds of scheme.

Why use χEFT?

- Chiral Perturbation Theory (χPT) is a low-energy theory where gluons and quarks can be replaced by effective degrees of freedom.
- χPT provides a formal expansion in terms of low-energy quark masses and momenta.
- The expansion is convergent if the quark masses and momenta are small enough so that higher-order terms are negligible. This is called the Power-Counting Regime (PCR).
- Within the PCR, χPT is renormalization scale-independent, and can be used to connect lattice simulations to the real world.
- Outside the PCR, χPT is, in general, scale-dependent, and care must be taken.
- Note: Here, we use 'χPT' to mean a massless renormalization scheme is used, but 'χEFT' allows different kinds of scheme.

Why use χEFT?

- Chiral Perturbation Theory (χPT) is a low-energy theory where gluons and quarks can be replaced by effective degrees of freedom.
- χPT provides a formal expansion in terms of low-energy quark masses and momenta.
- The expansion is convergent if the quark masses and momenta are small enough so that higher-order terms are negligible. This is called the Power-Counting Regime (PCR).
- Within the PCR, χPT is renormalization scale-independent, and can be used to connect lattice simulations to the real world.
- Outside the PCR, χPT is, in general, scale-dependent, and care must be taken.
- Note: Here, we use 'χPT' to mean a massless renormalization scheme is used, but 'χEFT' allows different kinds of scheme.

Why use χEFT?

- Chiral Perturbation Theory (χPT) is a low-energy theory where gluons and quarks can be replaced by effective degrees of freedom.
- χPT provides a formal expansion in terms of low-energy quark masses and momenta.
- The expansion is convergent if the quark masses and momenta are small enough so that higher-order terms are negligible. This is called the Power-Counting Regime (PCR).
- Within the PCR, χPT is renormalization scale-independent, and can be used to connect lattice simulations to the real world.
- Outside the PCR, χPT is, in general, scale-dependent, and care must be taken.
- Note: Here, we use 'χPT' to mean a massless renormalization scheme is used, but 'χEFT' allows different kinds of scheme.

Why use χEFT?

- Chiral Perturbation Theory (χPT) is a low-energy theory where gluons and quarks can be replaced by effective degrees of freedom.
- χPT provides a formal expansion in terms of low-energy quark masses and momenta.
- The expansion is convergent if the quark masses and momenta are small enough so that higher-order terms are negligible. This is called the Power-Counting Regime (PCR).
- Within the PCR, χPT is renormalization scale-independent, and can be used to connect lattice simulations to the real world.
- Outside the PCR, χPT is, in general, scale-dependent, and care must be taken.
- Note: Here, we use 'χPT' to mean a massless renormalization scheme is used, but 'χEFT' allows different kinds of scheme.

The PCR: Nucleon Mass

- The PCR is small; lattice results often extend outside the PCR.
- Example: The leading-order low-energy coefficients are held fixed for different regularization scales:

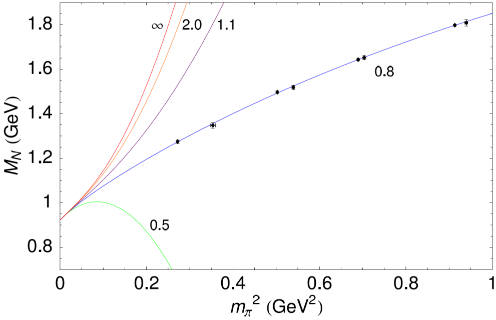

Chiral Effective Field Theory

Chiral Effective Field Theory

- For an effective field theory, one writes out a low-energy effective Lagrangian.
- The terms of the Lagrangian are ordered in powers of momenta and mass.
- For nucleons (fermions) written as an $\mathrm{SU}(2)$ doublet $\psi = (p \;\; n)^{\mathrm{T}}$, the relevant Lagrangian at $\mathcal{O}(p^4)$ takes the form:

$$\mathcal{L}_{\pi N}^{(1)} + \mathcal{L}_{tad}^{(2)} = \bar{\psi}\left(\not{\partial} - \overset{\circ}{M}_N + \frac{\overset{\circ}{g}_A}{2f_\pi}\gamma^\mu\gamma_5\vec{\tau}\cdot\partial_\mu\vec{\pi}\right)\psi + c_2\mathrm{Tr}[\mathcal{M}_+]\bar{\psi}\psi\,.$$

- The circle $\circ$ denotes a "bare" quantity: it becomes renormalized by chiral loops from the field theory. Let's look at the nucleon mass M_N ...

Chiral Effective Field Theory

- For an effective field theory, one writes out a low-energy effective Lagrangian.
- The terms of the Lagrangian are ordered in powers of momenta and mass.
- For nucleons (fermions) written as an $\mathrm{SU}(2)$ doublet $\psi = (p \;\; n)^{\mathrm{T}}$, the relevant Lagrangian at $\mathcal{O}(p^4)$ takes the form:

$$\mathcal{L}^{(1)}_{\pi N} + \mathcal{L}^{(2)}_{tad} = \bar{\psi}\left(\partial\!\!\!/ - \overset{\circ}{M}_N + \frac{\overset{\circ}{g}_A}{2f_\pi}\gamma^\mu\gamma_5\vec{\tau}\cdot\partial_\mu\vec{\pi}\right)\psi + c_2\mathrm{Tr}[\mathcal{M}_+]\bar{\psi}\psi\,.$$

- The circle $\circ$ denotes a "bare" quantity: it becomes renormalized by chiral loops from the field theory. Let's look at the nucleon mass M_N ...

Chiral Effective Field Theory

- For an effective field theory, one writes out a low-energy effective Lagrangian.
- The terms of the Lagrangian are ordered in powers of momenta and mass.
- For nucleons (fermions) written as an $\mathrm{SU}(2)$ doublet $\psi = (p \;\; n)^{\mathrm{T}}$, the relevant Lagrangian at $\mathcal{O}(p^4)$ takes the form:

$$\mathcal{L}_{\pi N}^{(1)} + \mathcal{L}_{tad}^{(2)} = \bar{\psi}\left(\not{\partial} - \overset{\circ}{M}_N + \frac{\overset{\circ}{g}_A}{2f_\pi}\gamma^\mu\gamma_5\vec{\tau}\cdot\partial_\mu\vec{\pi}\right)\psi + c_2 \mathrm{Tr}[\mathcal{M}_+]\bar{\psi}\psi\,.$$

- The circle $\circ$ denotes a “bare” quantity: it becomes renormalized by chiral loops from the field theory. Let's look at the nucleon mass M_N ...

Chiral Effective Field Theory

- For an effective field theory, one writes out a low-energy effective Lagrangian.
- The terms of the Lagrangian are ordered in powers of momenta and mass.
- For nucleons (fermions) written as an $\mathrm{SU}(2)$ doublet $\psi = (p \;\; n)^{\mathrm{T}}$, the relevant Lagrangian at $\mathcal{O}(p^4)$ takes the form:

$$\mathcal{L}_{\pi N}^{(1)} + \mathcal{L}_{tad}^{(2)} = \bar{\psi}\left(\not{\partial} - \mathring{M}_N + \frac{\mathring{g}_A}{2f_\pi}\gamma^\mu\gamma_5\vec{\tau}\cdot\partial_\mu\vec{\pi}\right)\psi + c_2\mathrm{Tr}[\mathcal{M}_+]\bar{\psi}\psi\,.$$

- The circle $\circ$ denotes a "bare" quantity: it becomes renormalized by chiral loops from the field theory. Let's look at the nucleon mass M_N ...

Chiral Effective Field Theory

- For an effective field theory, one writes out a low-energy effective Lagrangian.
- The terms of the Lagrangian are ordered in powers of momenta and mass.
- For nucleons (fermions) written as an $\mathrm{SU}(2)$ doublet $\psi = (p \;\; n)^{\mathrm{T}}$, the relevant Lagrangian at $\mathcal{O}(p^4)$ takes the form:

$$\mathcal{L}^{(1)}_{\pi N} + \mathcal{L}^{(2)}_{tad} = \bar{\psi}\left(\not{\partial} - \overset{\circ}{M}_N + \frac{\overset{\circ}{g}_A}{2f_\pi}\gamma^\mu\gamma_5\vec{\tau}\cdot\partial_\mu\vec{\pi}\right)\psi + c_2\mathrm{Tr}[\mathcal{M}_+]\bar{\psi}\psi\,.$$

- The circle $\circ$ denotes a "bare" quantity: it becomes renormalized by chiral loops from the field theory. Let's look at the nucleon mass M_N ...

Chiral Effective Field Theory

- Using the Gell-Mann—Oakes—Renner Relation, $m_q \propto m_\pi^2$, the nucleon mass M_N is renormalized by:

$$\begin{aligned} M_N &= \{\text{terms analytic in } m_\pi^2\} + \{\text{chiral loop corrections}\} \\ &= \{a_0 + a_2 m_\pi^2 + a_4 m_\pi^4 + \mathcal{O}(m_\pi^6)\} + \{\Sigma_{\text{loops}}\}\,. \end{aligned}$$

- The analytic coefficients a_i of the 'residual series' will be determined by fitting to lattice QCD results.
- The chiral loops have known, scale-independent coefficients, but given rise to non-analytic behaviour.

Chiral Effective Field Theory

- Using the Gell-Mann–Oakes–Renner Relation, $m_q \propto m_\pi^2$, the nucleon mass M_N is renormalized by:

$$\begin{aligned} M_N &= \{\text{terms analytic in } m_\pi^2\} + \{\text{chiral loop corrections}\} \\ &= \{a_0 + a_2 m_\pi^2 + a_4 m_\pi^4 + \mathcal{O}(m_\pi^6)\} + \{\Sigma_{\text{loops}}\}\,. \end{aligned}$$

- The analytic coefficients a_i of the 'residual series' will be determined by fitting to lattice QCD results.
- The chiral loops have known, scale-independent coefficients, but given rise to non-analytic behaviour.

Chiral Effective Field Theory

- Using the Gell-Mann—Oakes—Renner Relation, $m_q \propto m_\pi^2$, the nucleon mass M_N is renormalized by:

$$\begin{aligned} M_N &= \{\text{terms analytic in } m_\pi^2\} + \{\text{chiral loop corrections}\} \\ &= \{a_0 + a_2 m_\pi^2 + a_4 m_\pi^4 + \mathcal{O}(m_\pi^6)\} + \{\Sigma_{\text{loops}}\}\,. \end{aligned}$$

- The analytic coefficients a_i of the 'residual series' will be determined by fitting to lattice QCD results.
- The chiral loops have known, scale-independent coefficients, but given rise to non-analytic behaviour.

Chiral Effective Field Theory

- Using the Gell-Mann—Oakes—Renner Relation, $m_q \propto m_\pi^2$, the nucleon mass M_N is renormalized by:

$$\begin{aligned} M_N &= \{\text{terms analytic in } m_\pi^2\} + \{\text{chiral loop corrections}\} \\ &= \{a_0 + a_2 m_\pi^2 + a_4 m_\pi^4 + \mathcal{O}(m_\pi^6)\} + \{\Sigma_{\text{loops}}\}. \end{aligned}$$

- The analytic coefficients a_i of the 'residual series' will be determined by fitting to lattice QCD results.
- The chiral loops have known, scale-independent coefficients, but given rise to non-analytic behaviour.

Chiral Loops: Heavy Baryon Limit

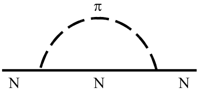

$$= \Sigma_N = \frac{\chi_N}{2\pi^2} \int \mathrm{d}^3 k \, \frac{k^2 u^2(k;\Lambda)}{\omega^2(k)} \quad \left(\omega(k) = \sqrt{k^2 + m_\pi^2}\right)$$

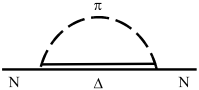

$$= \Sigma_\Delta = \frac{\chi_\Delta}{2\pi^2} \int \mathrm{d}^3 k \, \frac{k^2 u^2(k;\Lambda)}{\omega(k)(\Delta + \omega(k))} \quad (\Delta = M_\Delta - M_N)$$

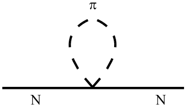

$$= \Sigma_{tad} = m_\pi^2 \frac{\chi_t'}{4\pi} \int \mathrm{d}^3 k \, \frac{2 u^2(k;\Lambda)}{\omega(k)}$$

‘Taylor’ Expansion of Chiral Loops

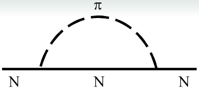

$$= \Sigma_N = b_0^N + b_2^N m_\pi^2 + \chi_N m_\pi^3 + b_4^N m_\pi^4 + \mathcal{O}(m_\pi^5)$$

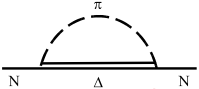

$$= \Sigma_\Delta = b_0^\Delta + b_2^\Delta m_\pi^2 + b_4^\Delta m_\pi^4 - \frac{3}{4\pi\Delta}\chi_\Delta m_\pi^4 \log \frac{m_\pi}{\mu} + \mathcal{O}(m_\pi^5)$$

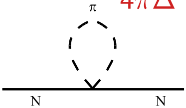

$$= \Sigma_{tad} = b_2^{t'} m_\pi^2 + b_4^{t'} m_\pi^4 + \chi_t' m_\pi^4 \log \frac{m_\pi}{\mu} + \mathcal{O}(m_\pi^5)$$

- Note: each integral expansion has an analytic polynomial, involving $b_i(\Lambda)$, and non-analytic terms.

Renormalization

- How does the renormalization take place?
  Consider the 1−pion loop integral as a test example:

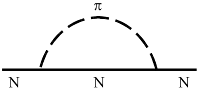

$$\Sigma_N = \frac{2\chi_N}{\pi}\int_0^\infty \mathrm{d}k\, \frac{k^4}{k^2+m_\pi^2}$$

$$= \frac{2\chi_N}{\pi}\int_0^\infty \mathrm{d}k\, \frac{(k^2+m_\pi^2)(k^2-m_\pi^2)+m_\pi^4}{k^2+m_\pi^2}$$

$$= \frac{2\chi_N}{\pi}\left(\int_0^\infty \mathrm{d}k\, k^2 - m_\pi^2\int_0^\infty \mathrm{d}k\right) + \chi_N m_\pi^3\,.$$

Renormalization

- How does the renormalization take place?
  Consider the 1−pion loop integral as a test example:

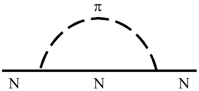

$$\Sigma_N = \frac{2\chi_N}{\pi}\int_0^\infty \mathrm{d}k \, \frac{k^4}{k^2+m_\pi^2}$$

$$= \frac{2\chi_N}{\pi}\int_0^\infty \mathrm{d}k \, \frac{(k^2+m_\pi^2)(k^2-m_\pi^2)+m_\pi^4}{k^2+m_\pi^2}$$

$$= \frac{2\chi_N}{\pi}\left(\int_0^\infty \mathrm{d}k\, k^2 - m_\pi^2\int_0^\infty \mathrm{d}k\right) + \chi_N m_\pi^3 \, .$$

Renormalization

- How does the renormalization take place?
  Consider the 1−pion loop integral as a test example:

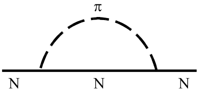

$$\Sigma_N = \frac{2\chi_N}{\pi}\int_0^\infty \mathrm{d}k\,\frac{k^4}{k^2+m_\pi^2}$$

$$= \frac{2\chi_N}{\pi}\int_0^\infty \mathrm{d}k\,\frac{(k^2+m_\pi^2)(k^2-m_\pi^2)+m_\pi^4}{k^2+m_\pi^2}$$

$$= \frac{2\chi_N}{\pi}\left(\int_0^\infty \mathrm{d}k\,k^2 - m_\pi^2\int_0^\infty \mathrm{d}k\right) + \chi_N m_\pi^3\,.$$

Renormalization

- How does the renormalization take place?
  Consider the 1−pion loop integral as a test example:

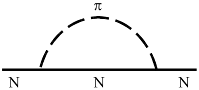

$$\Sigma_N = \frac{2\chi_N}{\pi}\int_0^\infty \mathrm{d}k \frac{k^4}{k^2+m_\pi^2}$$

$$= \frac{2\chi_N}{\pi}\int_0^\infty \mathrm{d}k \frac{(k^2+m_\pi^2)(k^2-m_\pi^2)+m_\pi^4}{k^2+m_\pi^2}$$

$$= \frac{2\chi_N}{\pi}\left(\int_0^\infty \mathrm{d}k\, k^2 - m_\pi^2\int_0^\infty \mathrm{d}k\right) + \chi_N m_\pi^3 .$$

Renormalization

- How does the renormalization take place?
  Consider the 1−pion loop integral as a test example:

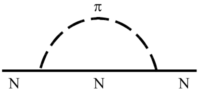

$$
\begin{aligned}
\Sigma_N &= \frac{2\chi_N}{\pi}\int_0^\infty \mathrm{d}k\,\frac{k^4}{k^2+m_\pi^2} \\
&= \frac{2\chi_N}{\pi}\int_0^\infty \mathrm{d}k\,\frac{(k^2+m_\pi^2)(k^2-m_\pi^2)+m_\pi^4}{k^2+m_\pi^2} \\
&= \frac{2\chi_N}{\pi}\left(\int_0^\infty \mathrm{d}k\,k^2 - m_\pi^2\int_0^\infty \mathrm{d}k\right) + \chi_N m_\pi^3\,.
\end{aligned}
$$

Renormalization

- In a massless renormalization scheme, there is no explicit momentum cutoff, so each of the a_i coefficients undergoes an infinite renormalization or none at all:

$$
\begin{aligned}
c_0 &= a_0 + \frac{2\chi_N}{\pi}\int_0^\infty \mathrm{d}k\, k^2\,, \\
c_2 &= a_2 - \frac{2\chi_N}{\pi}\int_0^\infty \mathrm{d}k\,, \\
c_4 &= a_4 + 0\,, \text{ etc.}
\end{aligned}
$$

Renormalization

- In a massless renormalization scheme, there is no explicit momentum cutoff, so each of the a_i coefficients undergoes an infinite renormalization or none at all:

$$
\begin{aligned}
c_0 &= a_0 + \frac{2\chi_N}{\pi}\int_0^\infty \mathrm{d}k\, k^2\,, \\
c_2 &= a_2 - \frac{2\chi_N}{\pi}\int_0^\infty \mathrm{d}k\,, \\
c_4 &= a_4 + 0\,, \ \text{etc.}
\end{aligned}
$$

Renormalization

- In a massless renormalization scheme, there is no explicit momentum cutoff, so each of the a_i coefficients undergoes an infinite renormalization or none at all:

$$
\begin{aligned}
c_0 &= a_0 + \frac{2\chi_N}{\pi}\int_0^\infty \mathrm{d}k\, k^2\,, \\
c_2 &= a_2 - \frac{2\chi_N}{\pi}\int_0^\infty \mathrm{d}k\,, \\
c_4 &= a_4 + 0\,, \ \text{etc.}
\end{aligned}
$$

Renormalization

- In a massless renormalization scheme, there is no explicit momentum cutoff, so each of the a_i coefficients undergoes an infinite renormalization or none at all:

$$
\begin{aligned}
c_0 &= a_0 + \frac{2\chi_N}{\pi}\int_0^\infty \mathrm{d}k\, k^2\,, \\
c_2 &= a_2 - \frac{2\chi_N}{\pi}\int_0^\infty \mathrm{d}k\,, \\
c_4 &= a_4 + 0\,, \ \text{etc.}
\end{aligned}
$$

Renormalization

- In Finite-Range Regularization (FRR), a finite momentum cutoff Λ is introduced (via a regulator function), and the chiral expansion is resummed.
- For a sharp cutoff regulator:

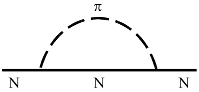

$$\begin{aligned}
\Sigma_N(\Lambda) &= \frac{2\chi_N}{\pi}\int_0^{\Lambda} \mathrm{d}k \frac{k^4}{k^2+m_\pi^2} \\
&= \frac{2\chi_N}{\pi}\left(\frac{\Lambda^3}{3} - \Lambda m_\pi^2 + m_\pi^3 \arctan\left[\frac{\Lambda}{m_\pi}\right]\right) \\
&= \frac{2\chi_N}{\pi}\frac{\Lambda^3}{3} - \frac{2\chi_N}{\pi}\Lambda m_\pi^2 + \chi_N m_\pi^3 - \frac{2\chi_N}{\pi}\frac{1}{\Lambda}m_\pi^4 + \cdots .
\end{aligned}$$

Renormalization

- In Finite-Range Regularization (FRR), a finite momentum cutoff Λ is introduced (via a regulator function), and the chiral expansion is resummed.
- For a sharp cutoff regulator:

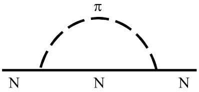

$$\begin{aligned}\Sigma_N(\Lambda) &= \frac{2\chi_N}{\pi}\int_0^\Lambda \mathrm{d}k\,\frac{k^4}{k^2+m_\pi^2}\\ &= \frac{2\chi_N}{\pi}\left(\frac{\Lambda^3}{3}-\Lambda m_\pi^2+m_\pi^3\arctan\left[\frac{\Lambda}{m_\pi}\right]\right)\\ &= \frac{2\chi_N}{\pi}\frac{\Lambda^3}{3}-\frac{2\chi_N}{\pi}\Lambda m_\pi^2+\chi_N m_\pi^3-\frac{2\chi_N}{\pi}\frac{1}{\Lambda}m_\pi^4+\cdots\,.\end{aligned}$$

Renormalization

- In Finite-Range Regularization (FRR), a finite momentum cutoff Λ is introduced (via a regulator function), and the chiral expansion is resummed.
- For a sharp cutoff regulator:

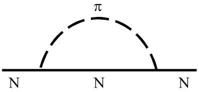

$$
\begin{aligned}
\Sigma_N(\Lambda) &= \frac{2\chi_N}{\pi}\int_0^{\Lambda} \mathrm{d}k \, \frac{k^4}{k^2+m_\pi^2} \\
&= \frac{2\chi_N}{\pi}\left(\frac{\Lambda^3}{3} - \Lambda m_\pi^2 + m_\pi^3 \arctan\left[\frac{\Lambda}{m_\pi}\right]\right) \\
&= \frac{2\chi_N}{\pi}\frac{\Lambda^3}{3} - \frac{2\chi_N}{\pi}\Lambda m_\pi^2 + \chi_N m_\pi^3 - \frac{2\chi_N}{\pi}\frac{1}{\Lambda}m_\pi^4 + \cdots \,.
\end{aligned}
$$

Renormalization

- In Finite-Range Regularization (FRR), a finite momentum cutoff Λ is introduced (via a regulator function), and the chiral expansion is resummed.
- For a sharp cutoff regulator:

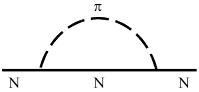

$$
\begin{aligned}
\Sigma_N(\Lambda) &= \frac{2\chi_N}{\pi}\int_0^{\Lambda}\mathrm{d}k\,\frac{k^4}{k^2+m_\pi^2} \\
&= \frac{2\chi_N}{\pi}\left(\frac{\Lambda^3}{3} - \Lambda m_\pi^2 + m_\pi^3\arctan\left[\frac{\Lambda}{m_\pi}\right]\right) \\
&= \frac{2\chi_N}{\pi}\frac{\Lambda^3}{3} - \frac{2\chi_N}{\pi}\Lambda m_\pi^2 + \chi_N m_\pi^3 - \frac{2\chi_N}{\pi}\frac{1}{\Lambda}m_\pi^4 + \cdots .
\end{aligned}
$$

Renormalization

- In Finite-Range Regularization (FRR), a finite momentum cutoff Λ is introduced (via a regulator function), and the chiral expansion is resummed.
- For a sharp cutoff regulator:

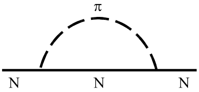

$$\begin{aligned}
\Sigma_N(\Lambda) &= \frac{2\chi_N}{\pi}\int_0^{\Lambda} \mathrm{d}k \frac{k^4}{k^2+m_\pi^2} \\
&= \frac{2\chi_N}{\pi}\left(\frac{\Lambda^3}{3} - \Lambda m_\pi^2 + m_\pi^3 \arctan\left[\frac{\Lambda}{m_\pi}\right]\right) \\
&= \frac{2\chi_N}{\pi}\frac{\Lambda^3}{3} - \frac{2\chi_N}{\pi}\Lambda m_\pi^2 + \chi_N m_\pi^3 - \frac{2\chi_N}{\pi}\frac{1}{\Lambda} m_\pi^4 + \cdots .
\end{aligned}$$

Renormalization

- The massless renormalization scheme result is recovered as $\Lambda \to \infty$.

$$
\begin{aligned}
c_0 &= a_0 + \frac{2\chi_N}{3}\Lambda^3\,, \\
c_2 &= a_2 - \frac{2\chi_N}{\pi}\Lambda\,, \\
c_4 &= a_4 - \frac{2\chi_N}{\pi}\frac{1}{\Lambda}\,, \text{ etc.}
\end{aligned}
$$

- The scale-dependence of the a_i's exactly compensates the scale-dependence of the b_i's, so each c_i is scale-independent, even at finite Λ.

Renormalization

- The massless renormalization scheme result is recovered as $\Lambda \to \infty$.

$$
\begin{aligned}
c_0 &= a_0 + \frac{2\chi_N}{3}\Lambda^3 \,, \\
c_2 &= a_2 - \frac{2\chi_N}{\pi}\Lambda \,, \\
c_4 &= a_4 - \frac{2\chi_N}{\pi}\frac{1}{\Lambda} \,, \text{ etc.}
\end{aligned}
$$

- The scale-dependence of the a_i's exactly compensates the scale-dependence of the b_i's, so each c_i is scale-independent, even at finite Λ.

Renormalization

- The massless renormalization scheme result is recovered as $\Lambda \to \infty$.

$$
\begin{aligned}
c_0 &= a_0 + \frac{2\chi_N}{3}\Lambda^3 \,, \\
c_2 &= a_2 - \frac{2\chi_N}{\pi}\Lambda \,, \\
c_4 &= a_4 - \frac{2\chi_N}{\pi}\frac{1}{\Lambda} \,, \ \text{etc.}
\end{aligned}
$$

- The scale-dependence of the a_i's exactly compensates the scale-dependence of the b_i's, so each c_i is scale-independent, even at finite Λ.

Renormalization

- The massless renormalization scheme result is recovered as $\Lambda \to \infty$.

$$
\begin{aligned}
c_0 &= a_0 + \frac{2\chi_N}{3}\Lambda^3\,, \\
c_2 &= a_2 - \frac{2\chi_N}{\pi}\Lambda\,, \\
c_4 &= a_4 - \frac{2\chi_N}{\pi}\frac{1}{\Lambda}\,, \text{ etc.}
\end{aligned}
$$

- The scale-dependence of the a_i's exactly compensates the scale-dependence of the b_i's, so each c_i is scale-independent, even at finite Λ.

Renormalization

- The massless renormalization scheme result is recovered as $\Lambda \to \infty$.

$$
\begin{aligned}
c_0 &= a_0 + \frac{2\chi_N}{3}\Lambda^3 \,, \\
c_2 &= a_2 - \frac{2\chi_N}{\pi}\Lambda \,, \\
c_4 &= a_4 - \frac{2\chi_N}{\pi}\frac{1}{\Lambda} \,, \text{ etc.}
\end{aligned}
$$

- The scale-dependence of the a_i's exactly compensates the scale-dependence of the b_i's, so each c_i is scale-independent, even at finite Λ.

Renormalization

- The coefficients χ_N , χ_Δ & χ'_t are known, scale-independent parameters (related to g_A, f_π, etc).
- The coefficients $b_i(\Lambda)$ however, are scale-dependent, but they occur at the relevant chiral orders to renormalize the residual series:

$$\begin{aligned} c_0 &= a_0 + b_0^N + b_0^\Delta \,, \\ c_2 &= a_2 + b_2^N + b_2^\Delta + b_2^{t'} \,, \\ c_4 &= a_4 + b_4^N + b_4^\Delta + b_4^{t'} \,, \text{ etc.} \end{aligned}$$

- These renormalized coefficients c_i are scale-independent.
- The following expansion will also take into account finite-volume corrections:

$$\begin{aligned} M_N &= c_0 + c_2 m_\pi^2 + \chi_N m_\pi^3 + c_4 m_\pi^4 \\ &+ \left(-\frac{3}{4\pi\Delta}\chi_\Delta + \chi'_t\right) m_\pi^4 \log\frac{m_\pi}{\mu} + \mathcal{O}(m_\pi^5) \,. \end{aligned}$$

Renormalization

- The coefficients χ_N , χ_Δ & χ'_t are known, scale-independent parameters (related to g_A, f_π, etc).
- The coefficients $b_i(\Lambda)$ however, are scale-dependent, but they occur at the relevant chiral orders to renormalize the residual series:

$$\begin{aligned} c_0 &= a_0 + b_0^N + b_0^\Delta \,, \\ c_2 &= a_2 + b_2^N + b_2^\Delta + b_2^{t'} \,, \\ c_4 &= a_4 + b_4^N + b_4^\Delta + b_4^{t'} \,, \text{ etc.} \end{aligned}$$

- These renormalized coefficients c_i are scale-independent.
- The following expansion will also take into account finite-volume corrections:

$$\begin{aligned} M_N &= c_0 + c_2 m_\pi^2 + \chi_N m_\pi^3 + c_4 m_\pi^4 \\ &+ \left(-\frac{3}{4\pi\Delta}\chi_\Delta + \chi'_t\right) m_\pi^4 \log\frac{m_\pi}{\mu} + \mathcal{O}(m_\pi^5)\,. \end{aligned}$$

Renormalization

- The coefficients χ_N , χ_Δ & χ_t' are known, scale-independent parameters (related to g_A, f_π, etc).
- The coefficients $b_i(\Lambda)$ however, are scale-dependent, but they occur at the relevant chiral orders to renormalize the residual series:

$$
\begin{aligned}
c_0 &= a_0 + b_0^N + b_0^\Delta \,, \\
c_2 &= a_2 + b_2^N + b_2^\Delta + b_2^{t'} \,, \\
c_4 &= a_4 + b_4^N + b_4^\Delta + b_4^{t'} \,, \text{ etc.}
\end{aligned}
$$

- These renormalized coefficients c_i are scale-independent.
- The following expansion will also take into account finite-volume corrections:

$$
\begin{aligned}
M_N &= c_0 + c_2 m_\pi^2 + \chi_N m_\pi^3 + c_4 m_\pi^4 \\
&+ \left(-\frac{3}{4\pi\Delta}\chi_\Delta + \chi_t'\right) m_\pi^4 \log\frac{m_\pi}{\mu} + \mathcal{O}(m_\pi^5) \,.
\end{aligned}
$$

Renormalization

- The coefficients χ_N , χ_Δ & χ'_t are known, scale-independent parameters (related to g_A, f_π, etc).
- The coefficients $b_i(\Lambda)$ however, are scale-dependent, but they occur at the relevant chiral orders to renormalize the residual series:

$$\begin{aligned} c_0 &= a_0 + b_0^N + b_0^\Delta \,, \\ c_2 &= a_2 + b_2^N + b_2^\Delta + b_2^{t'} \,, \\ c_4 &= a_4 + b_4^N + b_4^\Delta + b_4^{t'} \,, \ \text{etc.} \end{aligned}$$

- These renormalized coefficients c_i are scale-independent.
- The following expansion will also take into account finite-volume corrections:

$$\begin{aligned} M_N &= c_0 + c_2 m_\pi^2 + \chi_N m_\pi^3 + c_4 m_\pi^4 \\ &+ \left(-\frac{3}{4\pi\Delta}\chi_\Delta + \chi'_t\right) m_\pi^4 \log\frac{m_\pi}{\mu} + \mathcal{O}(m_\pi^5) \,. \end{aligned}$$

Renormalization

- The coefficients χ_N , χ_Δ & χ'_t are known, scale-independent parameters (related to g_A, f_π, etc).
- The coefficients $b_i(\Lambda)$ however, are scale-dependent, but they occur at the relevant chiral orders to renormalize the residual series:

$$\begin{aligned} c_0 &= a_0 + b_0^N + b_0^\Delta \,, \\ c_2 &= a_2 + b_2^N + b_2^\Delta + b_2^{t'} \,, \\ c_4 &= a_4 + b_4^N + b_4^\Delta + b_4^{t'} \,, \text{ etc.} \end{aligned}$$

- These renormalized coefficients c_i are scale-independent.
- The following expansion will also take into account finite-volume corrections:

$$\begin{aligned} M_N &= c_0 + c_2 m_\pi^2 + \chi_N m_\pi^3 + c_4 m_\pi^4 \\ &+ \left(-\frac{3}{4\pi\Delta}\chi_\Delta + \chi'_t\right) m_\pi^4 \log\frac{m_\pi}{\mu} + \mathcal{O}(m_\pi^5)\,. \end{aligned}$$

Renormalization

- The coefficients χ_N , χ_Δ & χ'_t are known, scale-independent parameters (related to g_A, f_π, etc).
- The coefficients $b_i(\Lambda)$ however, are scale-dependent, but they occur at the relevant chiral orders to renormalize the residual series:

$$\begin{aligned} c_0 &= a_0 + b_0^N + b_0^\Delta \,, \\ c_2 &= a_2 + b_2^N + b_2^\Delta + b_2^{t'} \,, \\ c_4 &= a_4 + b_4^N + b_4^\Delta + b_4^{t'} \,, \text{ etc.} \end{aligned}$$

- These renormalized coefficients c_i are scale-independent.
- The following expansion will also take into account finite-volume corrections:

$$\begin{aligned} M_N &= c_0 + c_2 m_\pi^2 + \chi_N m_\pi^3 + c_4 m_\pi^4 \\ &+ \left(-\frac{3}{4\pi\Delta}\chi_\Delta + \chi'_t\right) m_\pi^4 \log\frac{m_\pi}{\mu} + \mathcal{O}(m_\pi^5) \,. \end{aligned}$$

Renormalization

- The coefficients χ_N , χ_Δ & χ'_t are known, scale-independent parameters (related to g_A, f_π, etc).
- The coefficients $b_i(\Lambda)$ however, are scale-dependent, but they occur at the relevant chiral orders to renormalize the residual series:

$$\begin{aligned} c_0 &= a_0 + b_0^N + b_0^\Delta \,, \\ c_2 &= a_2 + b_2^N + b_2^\Delta + b_2^{t'} \,, \\ c_4 &= a_4 + b_4^N + b_4^\Delta + b_4^{t'} \,, \text{ etc.} \end{aligned}$$

- These renormalized coefficients c_i are scale-independent.
- The following expansion will also take into account finite-volume corrections:

$$\begin{aligned} M_N &= c_0 + c_2 m_\pi^2 + \chi_N m_\pi^3 + c_4 m_\pi^4 \\ &+ \left(-\frac{3}{4\pi\Delta}\chi_\Delta + \chi'_t\right) m_\pi^4 \log\frac{m_\pi}{\mu} + \mathcal{O}(m_\pi^5)\,. \end{aligned}$$

Finite-Range Regulators

- Recall:

$$\Sigma_N = \frac{\chi_N}{2\pi^2} \int \mathrm{d}^3k \, \frac{k^2 u^2(k;\Lambda)}{\omega^2(k)}.$$

- All forms of $u(k;\Lambda)$ are equivalent within the PCR.
- Consider the family of smooth $n-$tuple dipole attenuators:

$$u_n(k;\Lambda) = \left(1 + \frac{k^{2n}}{\Lambda^{2n}}\right)^{-2}.$$

- The dipole corresponds to $n = 1$. We shall also consider the cases $n = 2, 3$, the double- and triple-dipole forms, respectively.

Finite-Range Regulators

- Recall:

$$\Sigma_N = \frac{\chi_N}{2\pi^2}\int \mathrm{d}^3k\,\frac{k^2 u^2(k;\Lambda)}{\omega^2(k)}.$$

- All forms of $u(k;\Lambda)$ are equivalent within the PCR.
- Consider the family of smooth $n-$tuple dipole attenuators:

$$u_n(k;\Lambda) = \left(1 + \frac{k^{2n}}{\Lambda^{2n}}\right)^{-2}.$$

- The dipole corresponds to $n = 1$. We shall also consider the cases $n = 2, 3$, the double- and triple-dipole forms, respectively.

Finite-Range Regulators

- Recall:

$$\Sigma_N = \frac{\chi_N}{2\pi^2}\int \mathrm{d}^3k\,\frac{k^2 u^2(k;\Lambda)}{\omega^2(k)}.$$

- All forms of $u(k;\Lambda)$ are equivalent within the PCR.
- Consider the family of smooth $n-$tuple dipole attenuators:

$$u_n(k;\Lambda) = \left(1 + \frac{k^{2n}}{\Lambda^{2n}}\right)^{-2}.$$

- The dipole corresponds to $n = 1$. We shall also consider the cases $n = 2, 3$, the double- and triple-dipole forms, respectively.

Finite-Range Regulators

- Recall:

$$\Sigma_N = \frac{\chi_N}{2\pi^2} \int \mathrm{d}^3k \, \frac{k^2 u^2(k;\Lambda)}{\omega^2(k)}.$$

- All forms of $u(k;\Lambda)$ are equivalent within the PCR.
- Consider the family of smooth $n-$tuple dipole attenuators:

$$u_n(k;\Lambda) = \left(1 + \frac{k^{2n}}{\Lambda^{2n}}\right)^{-2}.$$

- The dipole corresponds to $n = 1$. We shall also consider the cases $n = 2, 3$, the double- and triple-dipole forms, respectively.

Finite-Range Regulators

- Recall:

$$\Sigma_N = \frac{\chi_N}{2\pi^2}\int \mathrm{d}^3k\,\frac{k^2 u^2(k;\Lambda)}{\omega^2(k)}.$$

- All forms of $u(k;\Lambda)$ are equivalent within the PCR.
- Consider the family of smooth $n-$tuple dipole attenuators:

$$u_n(k;\Lambda) = \left(1 + \frac{k^{2n}}{\Lambda^{2n}}\right)^{-2}.$$

- The dipole corresponds to $n = 1$. We shall also consider the cases $n = 2, 3$, the double- and triple-dipole forms, respectively.

Finite-Range Regulators

- Here are the three dipole-like forms at $\Lambda = 1.0$ GeV:

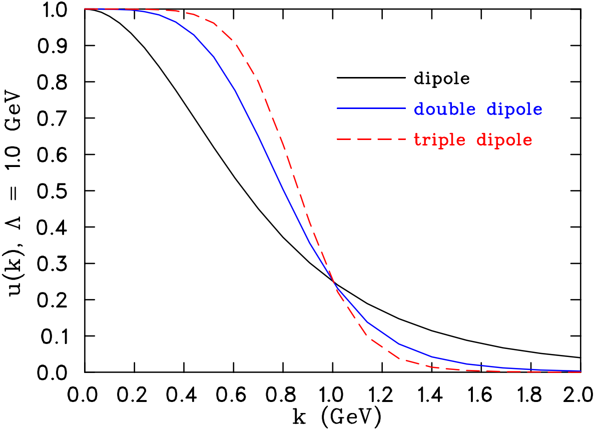

Lattice QCD Simulation Results

- In investigating the nucleon mass, we use lattice QCD results from:
  - PACS-CS (2009), arXiv:0807.1661v1: non-perturbatively $\mathcal{O}(a)$-improved Wilson quarks, $L = 2.9$ fm.
  - JLQCD (2008), arXiv:0806.4744v3: $N_f = 2$ overlap fermions at $L = 1.9$ fm.
  - CP-PACS (2002), arXiv:hep-lat/0105015v1: mean field improved clover quark action at $L = 2.2 \to 2.8$ fm.

Intrinsic Scale Model: Pseudodata Analysis

Trial Extrapolations

- Consider an extrapolation of results from PACS-CS, using a dipole regulator with $\Lambda_{\rm dip} = 1.0$ GeV.
- (PACS-CS: non-perturbatively $\mathcal{O}(a)$-improved Wilson quarks, $L = 2.9$ fm).

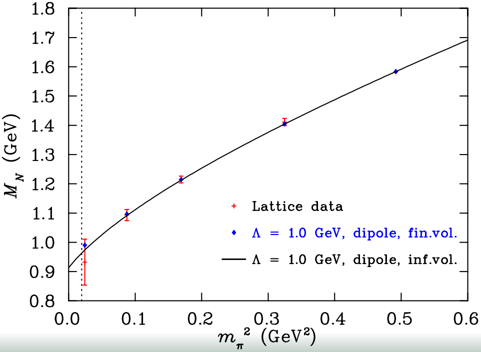

Trial Extrapolations

- Consider an extrapolation of results from CP-PACS, using a dipole regulator with $\Lambda_{\rm dip} = 1.0$ GeV.
- (CP-PACS: mean field improved clover quark action at $L = 2.2 \to 2.8$ fm).

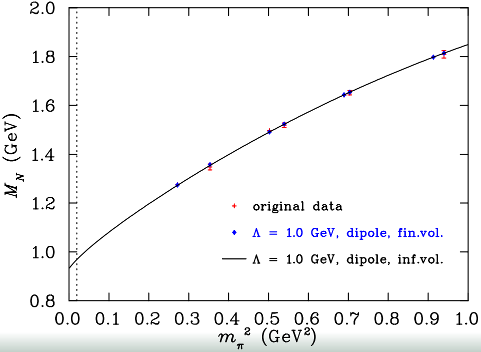

Trial Extrapolations

- What happens to the extrapolation as $\Lambda_{\rm dip}$ is changed?

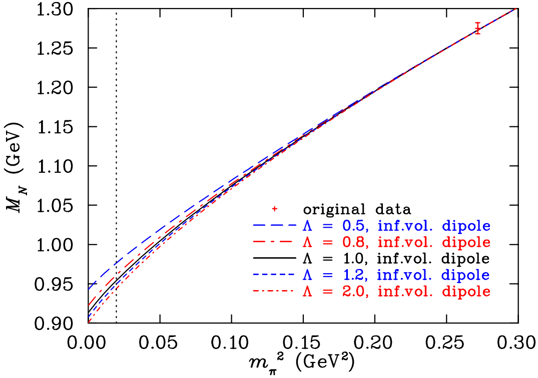

Pseudodata

- Different choices of regulator give different results! But is there an optimal choice?
- If we want to stay close to the PCR, how many data points should we use? Does it matter?
- Let's do a test: generate some ideal 'pseudodata' (infinite volume), at $\Lambda^{\text{created}} = 1.0$ GeV.
- As we increase the fit window, ie. increase the maximum m_π^2, does the scale-dependence of the result change?

Pseudodata

- Different choices of regulator give different results! But is there an optimal choice?
- If we want to stay close to the PCR, how many data points should we use? Does it matter?
- Let's do a test: generate some ideal 'pseudodata' (infinite volume), at $\Lambda^{\text{created}} = 1.0$ GeV.
- As we increase the fit window, ie. increase the maximum m_π^2, does the scale-dependence of the result change?

Pseudodata

- Different choices of regulator give different results! But is there an optimal choice?
- If we want to stay close to the PCR, how many data points should we use? Does it matter?
- Let's do a test: generate some ideal 'pseudodata' (infinite volume), at $\Lambda^{\text{created}} = 1.0$ GeV.
- As we increase the fit window, ie. increase the maximum m_π^2, does the scale-dependence of the result change?

Pseudodata

- Different choices of regulator give different results! But is there an optimal choice?
- If we want to stay close to the PCR, how many data points should we use? Does it matter?
- Let's do a test: generate some ideal 'pseudodata' (infinite volume), at $\Lambda^{\text{created}} = 1.0$ GeV.
- As we increase the fit window, ie. increase the maximum m_π^2, does the scale-dependence of the result change?

Pseudodata: Procedure

- Assume there is an 'intrinsic scale'.
- Create some ideal pseudodata using this scale.
- Develop a technique to recover the scale from the pseudodata.
- Later: apply to actual lattice results.

Pseudodata: Procedure

- Assume there is an 'intrinsic scale'.
- Create some ideal pseudodata using this scale.
- Develop a technique to recover the scale from the pseudodata.
- Later: apply to actual lattice results.

Pseudodata: Procedure

- Assume there is an ‘intrinsic scale’.
- Create some ideal pseudodata using this scale.
- Develop a technique to recover the scale from the pseudodata.
- Later: apply to actual lattice results.

Pseudodata: Procedure

- Assume there is an 'intrinsic scale'.
- Create some ideal pseudodata using this scale.
- Develop a technique to recover the scale from the pseudodata.
- Later: apply to actual lattice results.

Pseudodata: Renormalization Flow

- Consider the best fit c_0(GeV) renormalization flow.
- Notice that the correct value of c_0 is recovered exactly when $\Lambda_{\rm dip} = \Lambda_{\rm dip}^{\rm created}$.

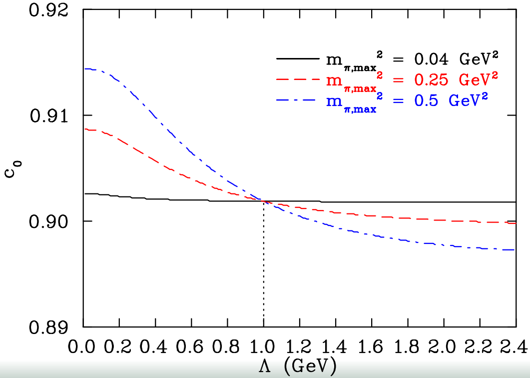

Pseudodata: Renormalization Flow

- Consider the best fit c_0(GeV) renormalization flow.
- Notice that the correct value of c_0 is recovered exactly when $\Lambda_{\rm dip} = \Lambda_{\rm dip}^{\rm created}$.

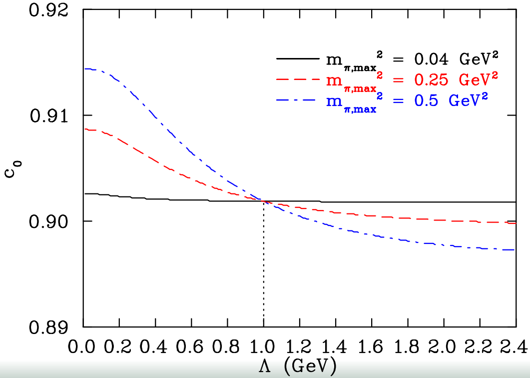

Pseudodata: Renormalization Flow

- Consider the result for c_2.
- Though it is tempting to read off the value of any c_i as $\Lambda \to \infty$, it is wrong (unless constrained to the PCR).

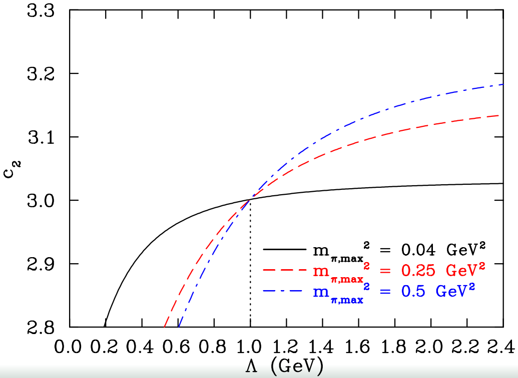

Pseudodata: Renormalization Flow

- Consider the result for c_2.
- Though it is tempting to read off the value of any c_i as $\Lambda \to \infty$, it is wrong (unless constrained to the PCR).

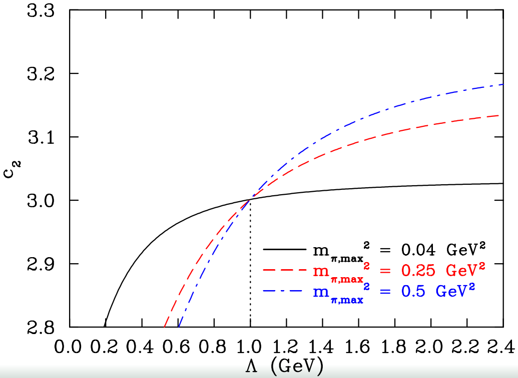

Pseudodata: Renormalization Flow

- This intersection point is not trivial. To demonstrate this, we can analyze the pseudodata using a triple-dipole.

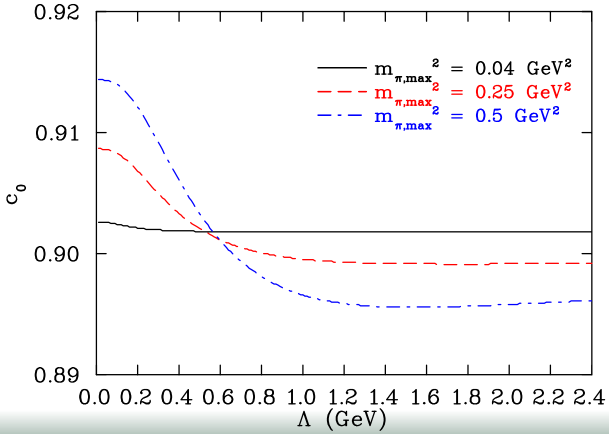

Pseudodata: Renormalization Flow

- The intersection is no longer a clear point, but a cluster at $\Lambda_{\text{dip}} \approx 0.5 - 0.6$ GeV. This is the preferred value of Λ_{trip}.

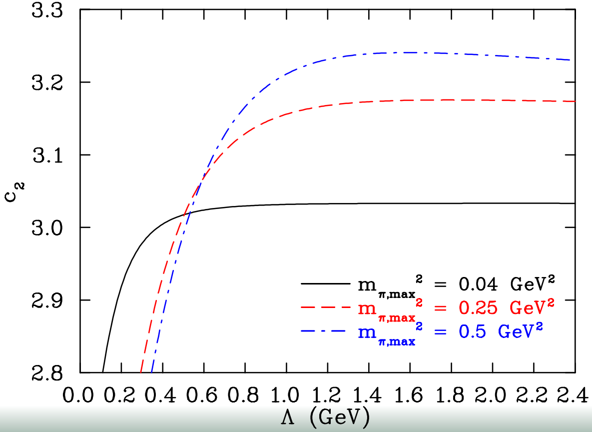

Intrinsic Scale: Mass of the Nucleon

Evidence for an Intrinsic Scale

- In the pseudodata test example, the optimal cutoff (by construction) was recovered from the pseudodata themselves.
- But do actual lattice QCD simulation results have an intrinsic scale embedded in them?
- One might investigate this possibility by searching for an optimal regularization scale associated with lattice results that extend beyond the PCR.

Evidence for an Intrinsic Scale

- In the pseudodata test example, the optimal cutoff (by construction) was recovered from the pseudodata themselves.
- But do actual lattice QCD simulation results have an intrinsic scale embedded in them?
- One might investigate this possibility by searching for an optimal regularization scale associated with lattice results that extend beyond the PCR.

Evidence for an Intrinsic Scale

- In the pseudodata test example, the optimal cutoff (by construction) was recovered from the pseudodata themselves.
- But do actual lattice QCD simulation results have an intrinsic scale embedded in them?
- One might investigate this possibility by searching for an optimal regularization scale associated with lattice results that extend beyond the PCR.

Evidence for an Intrinsic Scale

- Let us repeat our analysis for real lattice QCD results (eg. JLQCD results: $N_f = 2$ overlap fermions at $L = 1.9$ fm):

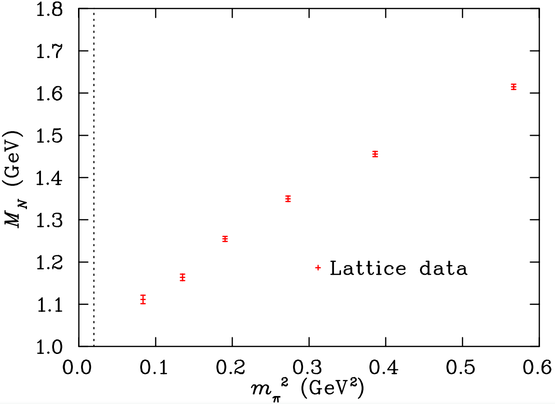

Evidence for an Intrinsic Scale

- Consider the renormalization flow for best fit c_0(GeV) using JLQCD results, working to chiral order $\mathcal{O}(m_\pi^3)$ and using a dipole regulator:

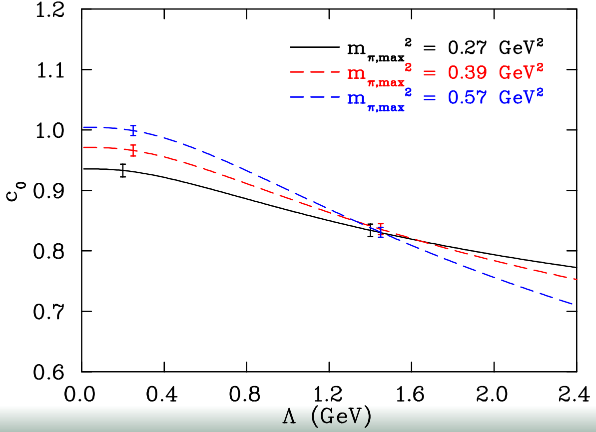

Evidence for an Intrinsic Scale

- The intersection occurs at the same value of Λ for both c_0 and c_2. This is a highly significant result:

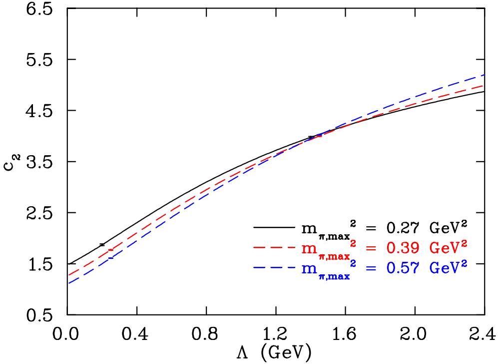

- To obtain a quantitative measure of the intrinsic scale, with an estimate of its systematic uncertainty, apply a χ^2_{dof}-style analysis...

Systematic Uncertainty

- Example plot: χ^2_{dof} obtained from c_0 using JLQCD results, working to chiral order $\mathcal{O}(m_\pi^3)$ and using a dipole regulator:

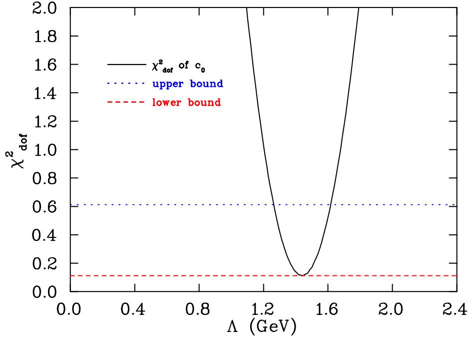

$$\chi^2_{dof} = \frac{1}{n-1} \sum_i \frac{[c(m^2_{\pi,\mathrm{max},i}\,;\Lambda) - \bar{c}(\Lambda)]^2}{[\delta c(m^2_{\pi,\mathrm{max},i}\,;\Lambda)]^2}.$$

Results

- The intrinsic scales $\Lambda^{\rm scale}$ (GeV) are tabulated for three different regulators and three different lattice result sets:

	regulator form		
optimal scale	dipole	double	triple
$\Lambda^{\rm scale}_{c_0,\rm JLQCD}$	$1.44^{+0.18}_{-0.18}$	$1.08^{+0.11}_{-0.11}$	$0.96^{+0.09}_{-0.09}$
$\Lambda^{\rm scale}_{c_2,\rm JLQCD}$	$1.40^{+0.02}_{-0.03}$	$1.05^{+0.02}_{-0.01}$	$0.94^{+0.01}_{-0.02}$
$\Lambda^{\rm scale}_{c_0,\rm PACS-CS}$	$1.21^{+0.66}_{-0.82}$	$0.93^{+0.41}_{-0.58}$	$0.83^{+0.35}_{-0.50}$
$\Lambda^{\rm scale}_{c_2,\rm PACS-CS}$	$1.21^{+0.18}_{-0.18}$	$0.93^{+0.11}_{-0.12}$	$0.83^{+0.10}_{-0.10}$
$\Lambda^{\rm scale}_{c_0,\rm CP-PACS}$	$1.20^{+0.10}_{-0.10}$	$0.98^{+0.06}_{-0.07}$	$0.88^{+0.06}_{-0.06}$
$\Lambda^{\rm scale}_{c_2,\rm CP-PACS}$	$1.19^{+0.02}_{-0.01}$	$0.97^{+0.01}_{-0.01}$	$0.87^{+0.01}_{-0.01}$

Nucleon Mass Summary

- The renormalization curves for different m_π^2 fit windows intersect at a well-defined point.
- This is true for a variety of regulators.
- In each case, c_0 and c_2 agree on the intrinsic scale: Λ^{scale}.
- This indicates that lattice QCD results provide guidance in selecting an optimal scale for χEFT beyond the PCR.

Nucleon Mass Summary

- The renormalization curves for different m_π^2 fit windows intersect at a well-defined point.
- This is true for a variety of regulators.
- In each case, c_0 and c_2 agree on the intrinsic scale: Λ^{scale}.
- This indicates that lattice QCD results provide guidance in selecting an optimal scale for χEFT beyond the PCR.

Nucleon Mass Summary

- The renormalization curves for different m_π^2 fit windows intersect at a well-defined point.
- This is true for a variety of regulators.
- In each case, c_0 and c_2 agree on the intrinsic scale: Λ^{scale}.
- This indicates that lattice QCD results provide guidance in selecting an optimal scale for χEFT beyond the PCR.

Nucleon Mass Summary

- The renormalization curves for different m_π^2 fit windows intersect at a well-defined point.
- This is true for a variety of regulators.
- In each case, c_0 and c_2 agree on the intrinsic scale: $\Lambda^{\rm scale}$.
- This indicates that lattice QCD results provide guidance in selecting an optimal scale for χEFT beyond the PCR.

Intrinsic Scale: Testing Robustness

Establishing a Robust Method: A Test

- Consider the quenched ρ meson.
- **The Challenge:** We want to predict the mass of the quenched ρ meson at physical pion mass ($m_{\pi,\mathrm{phys}} = 140$ MeV).
- We have quenched lattice QCD (QQCD) results from the Kentucky Group, but we are blinded to the lowest energy results.
- QQCD observables are an important testing ground, since there are no experimentally known values that can introduce a prejudice in the final result.

Establishing a Robust Method: A Test

- Consider the quenched ρ meson.
- **The Challenge:** We want to predict the mass of the quenched ρ meson at physical pion mass ($m_{\pi,\mathrm{phys}} = 140$ MeV).
- We have quenched lattice QCD (QQCD) results from the Kentucky Group, but we are blinded to the lowest energy results.
- QQCD observables are an important testing ground, since there are no experimentally known values that can introduce a prejudice in the final result.

Establishing a Robust Method: A Test

- Consider the quenched ρ meson.
- **The Challenge:** We want to predict the mass of the quenched ρ meson at physical pion mass ($m_{\pi,\mathrm{phys}} = 140$ MeV).
- We have quenched lattice QCD (QQCD) results from the Kentucky Group, but we are blinded to the lowest energy results.
- QQCD observables are an important testing ground, since there are no experimentally known values that can introduce a prejudice in the final result.

Establishing a Robust Method: A Test

- Consider the quenched ρ meson.
- **The Challenge:** We want to predict the mass of the quenched ρ meson at physical pion mass ($m_{\pi,\mathrm{phys}} = 140$ MeV).
- We have quenched lattice QCD (QQCD) results from the Kentucky Group, but we are blinded to the lowest energy results.
- QQCD observables are an important testing ground, since there are no experimentally known values that can introduce a prejudice in the final result.

QQCD Results from the Lattice

- The following results from Kentucky Group ($L = 3.06$ fm) are missing points close to the chiral limit.
- The available results lie in the range $380 < m_\pi < 1153$ MeV,
- The unavailable results lie in the range $200 < m_\pi < 380$ MeV.

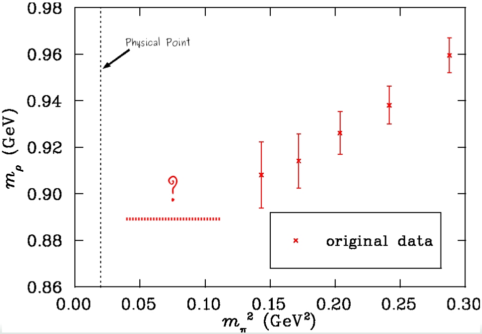

QQCD Results from the Lattice

- The following results from Kentucky Group ($L = 3.06$ fm) are missing points close to the chiral limit.
- The available results lie in the range $380 < m_\pi < 1153$ MeV,
- The unavailable results lie in the range $200 < m_\pi < 380$ MeV.

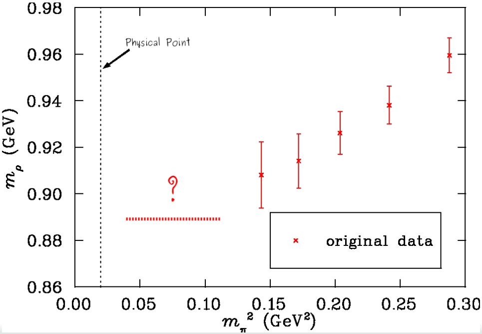

QQCD Results from the Lattice

- The following results from Kentucky Group ($L = 3.06$ fm) are missing points close to the chiral limit.
- The available results lie in the range $380 < m_\pi < 1153$ MeV,
- The unavailable results lie in the range $200 < m_\pi < 380$ MeV.

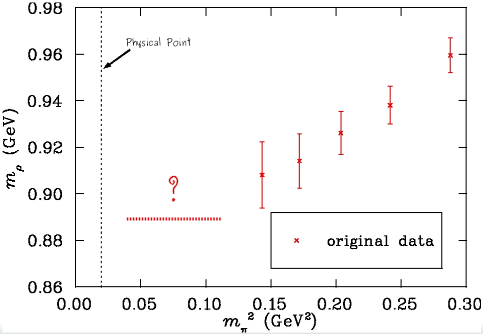

Chiral Extrapolation Formulae

- The quenched ρ meson mass expansion similarly contains a residual series and loop integrals.
- We will work to chiral order $\mathcal{O}(m_\pi^4)$.
- The renormalization of the low-energy constants takes place just as before. The fit parameters are a_0, a_2 and a_4.

Chiral Extrapolation Formulae

- The quenched ρ meson mass expansion similarly contains a residual series and loop integrals.
- We will work to chiral order $\mathcal{O}(m_\pi^4)$.
- The renormalization of the low-energy constants takes place just as before. The fit parameters are a_0, a_2 and a_4.

Chiral Extrapolation Formulae

- The quenched ρ meson mass expansion similarly contains a residual series and loop integrals.
- We will work to chiral order $\mathcal{O}(m_\pi^4)$.
- The renormalization of the low-energy constants takes place just as before. The fit parameters are a_0, a_2 and a_4.

Test for an Intrinsic Scale

- Consider the renormalization flow for c_0 using Kentucky Group results, working to chiral order $\mathcal{O}(m_\pi^4)$ and using a triple-dipole regulator:

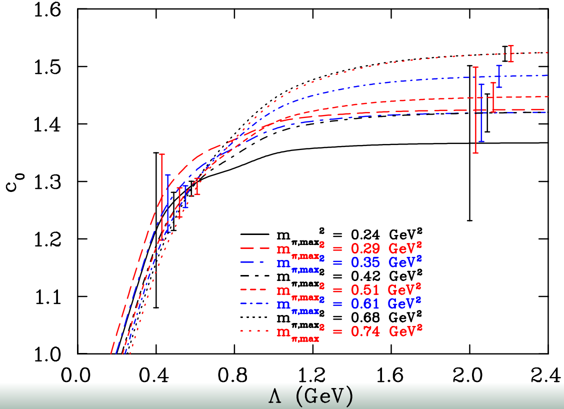

Test for an Intrinsic Scale

- The crossings are much harder to identify, so we will rely on our χ^2_{dof} method:

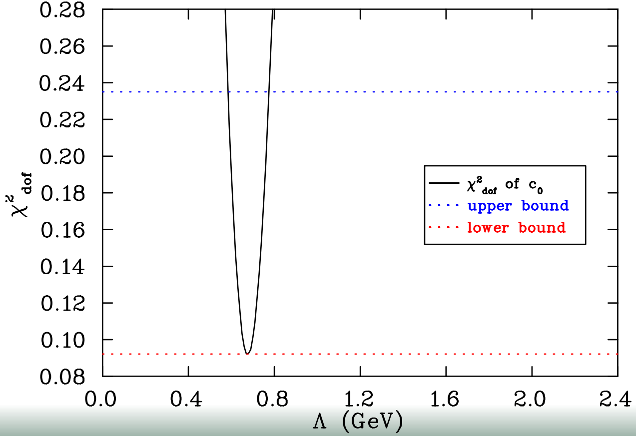

Test for an Intrinsic Scale

- Consider the result for c_2 using Kentucky Group results, working to chiral order $\mathcal{O}(m_\pi^4)$ and using a triple-dipole regulator:

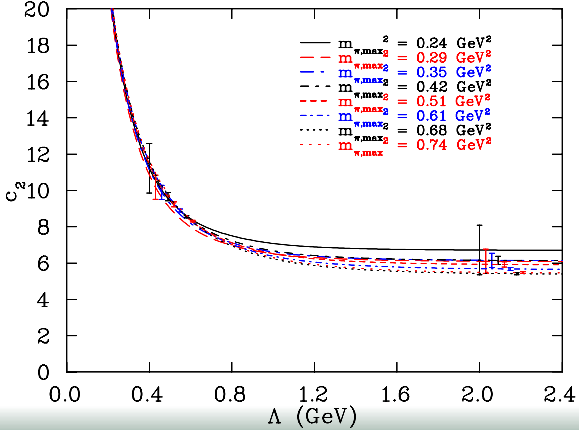

Test for an Intrinsic Scale

- Consider the result for c_4 using Kentucky Group results, working to chiral order $\mathcal{O}(m_\pi^4)$ and using a triple-dipole regulator:

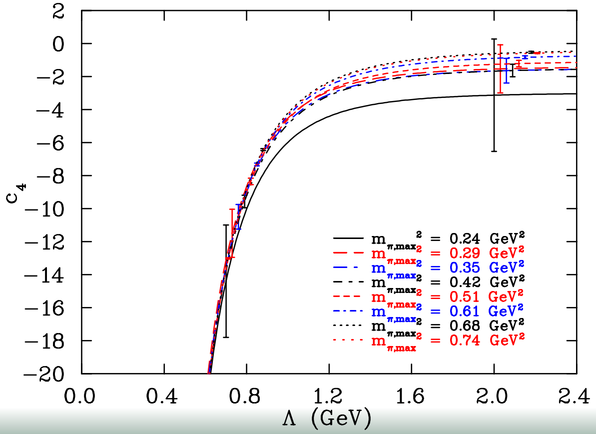

Test for an Intrinsic Scale

- The central, upper and lower regularization scales obtained from the χ^2_{dof} for the low-energy constants c_i:

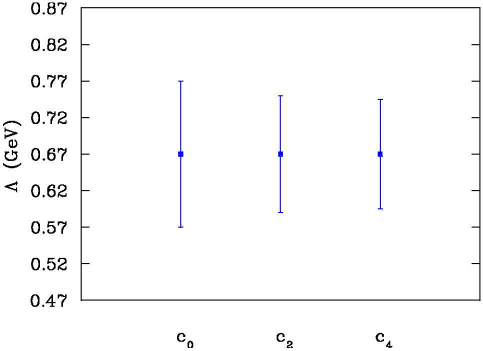

- The average value for the optimal regularization scale is: $\Lambda^{\rm scale} = 0.67^{+0.09}_{-0.08}$ GeV.

Completing 'The Challenge'

- $\Lambda^{\text{scale}} = 0.67^{+0.09}_{-0.08}$ GeV.
- Inner error bar: systematic error from parameters.
- Outer error bar: systematic and statistical errors in quadrature.

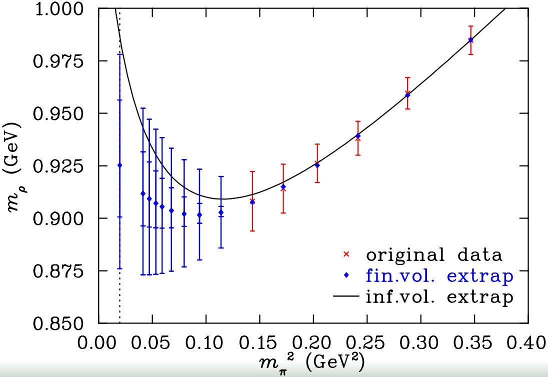

Completing 'The Challenge'

- $\Lambda^{\text{scale}} = 0.67^{+0.09}_{-0.08}$ GeV.
- Now, compare the low-energy lattice results (red):

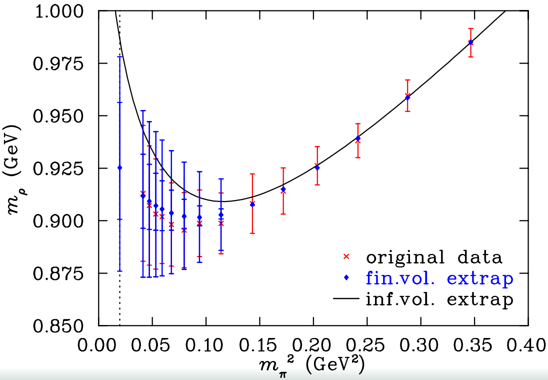

Completing ‘The Challenge’

- $\Lambda^{\mathrm{scale}} = 0.67^{+0.09}_{-0.08}$ GeV.
- Here, the error bars are correlated relative to the lightest data point in the original set, $m_\pi^2 = 0.143$ GeV^2.

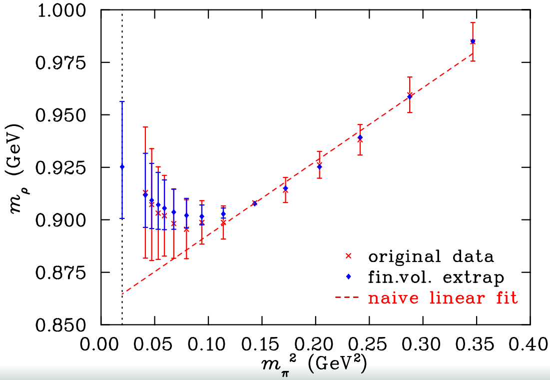

Including the Low-Energy Results

- By using the low-energy results within the PCR, scale-independence is recovered:

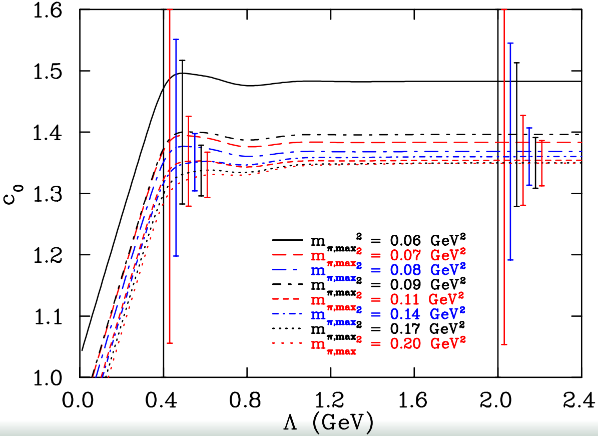

Including the Low-Energy Results

- By using the low-energy results within the PCR, scale-independence is recovered:

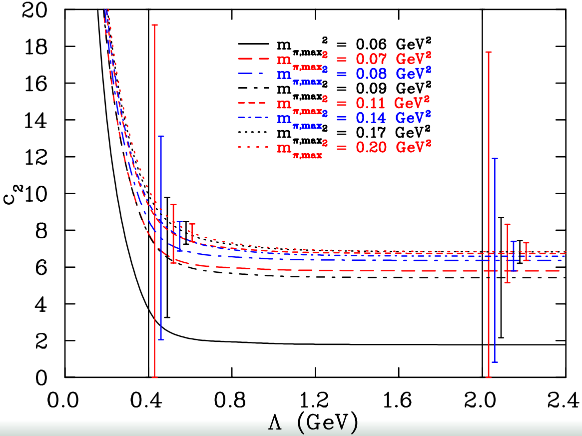

Including the Low-Energy Results

- By using the low-energy results within the PCR, scale-independence is recovered:

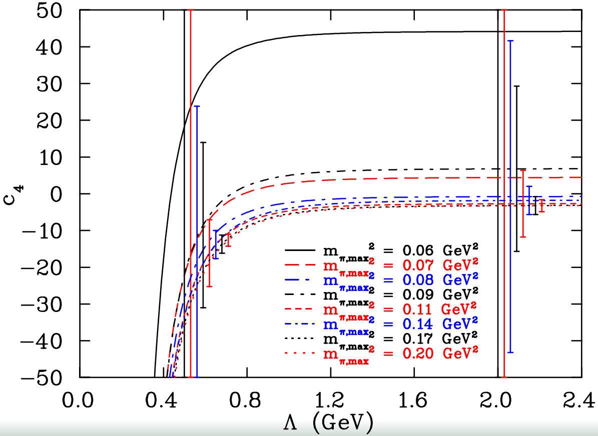

Optimal Fit Window

- Consider the renormalization of c_0 using the low-energy results.
- We can arbitrarily constrain the estimate of the systematic uncertainty from χ^2_{dof} by including more lattice results:

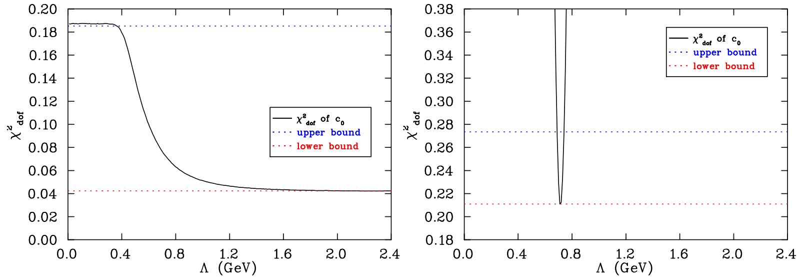

- *Left:* χ^2_{dof} using 11 points, *Right:* χ^2_{dof} using 17 points.

Optimal Fit Window

- How many data points should we include?
- Using a small number of results, extrapolation uncertainty is dominated by statistical error.
  - There are not enough results to constrain the fit parameters precisely.
- Using a large number of results, extrapolation uncertainty is dominated by systematic error.
  - There is greater scale-dependence using results that extend futher outside the PCR.
  - Extrapolation is, in general, more sensitive to changes in the parameters of the loop integrals.
- There should be an optimal value of $m^2_{\pi,\mathrm{max}}$, where the total uncertainty is minimized.

Optimal Fit Window

- How many data points should we include?
- Using a small number of results, extrapolation uncertainty is dominated by statistical error.
  - There are not enough results to constrain the fit parameters precisely.
- Using a large number of results, extrapolation uncertainty is dominated by systematic error.
  - There is greater scale-dependence using results that extend futher outside the PCR.
  - Extrapolation is, in general, more sensitive to changes in the parameters of the loop integrals.
- There should be an optimal value of $m^2_{\pi,\max}$, where the total uncertainty is minimized.

Optimal Fit Window

- How many data points should we include?
- Using a small number of results, extrapolation uncertainty is dominated by statistical error.
  - There are not enough results to constrain the fit parameters precisely.
- Using a large number of results, extrapolation uncertainty is dominated by systematic error.
  - There is greater scale-dependence using results that extend futher outside the PCR.
  - Extrapolation is, in general, more sensitive to changes in the parameters of the loop integrals.
- There should be an optimal value of $m^2_{\pi,\max}$, where the total uncertainty is minimized.

Optimal Fit Window

- How many data points should we include?
- Using a small number of results, extrapolation uncertainty is dominated by statistical error.
    - There are not enough results to constrain the fit parameters precisely.
- Using a large number of results, extrapolation uncertainty is dominated by systematic error.
    - There is greater scale-dependence using results that extend futher outside the PCR.
    - Extrapolation is, in general, more sensitive to changes in the parameters of the loop integrals.
- There should be an optimal value of $m^2_{\pi,\mathrm{max}}$, where the total uncertainty is minimized.

Optimal Fit Window

- How many data points should we include?
- Using a small number of results, extrapolation uncertainty is dominated by statistical error.
  - There are not enough results to constrain the fit parameters precisely.
- Using a large number of results, extrapolation uncertainty is dominated by systematic error.
  - There is greater scale-dependence using results that extend futher outside the PCR.
  - Extrapolation is, in general, more sensitive to changes in the parameters of the loop integrals.
- There should be an optimal value of $m^2_{\pi,\mathrm{max}}$, where the total uncertainty is minimized.

Optimal Fit Window

- How many data points should we include?
- Using a small number of results, extrapolation uncertainty is dominated by statistical error.
  - There are not enough results to constrain the fit parameters precisely.
- Using a large number of results, extrapolation uncertainty is dominated by systematic error.
  - There is greater scale-dependence using results that extend futher outside the PCR.
  - Extrapolation is, in general, more sensitive to changes in the parameters of the loop integrals.
- There should be an optimal value of $m^2_{\pi,\mathrm{max}}$, where the total uncertainty is minimized.

Optimal Fit Window

- How many data points should we include?
- Using a small number of results, extrapolation uncertainty is dominated by statistical error.
  - There are not enough results to constrain the fit parameters precisely.
- Using a large number of results, extrapolation uncertainty is dominated by systematic error.
  - There is greater scale-dependence using results that extend futher outside the PCR.
  - Extrapolation is, in general, more sensitive to changes in the parameters of the loop integrals.
- There should be an optimal value of $m^2_{\pi,\mathrm{max}}$, where the total uncertainty is minimized.

Optimal Fit Window

- Consider the extrapolation of m_ρ to the physical point as $m^2_{\pi,\mathrm{max}}$ is increased:

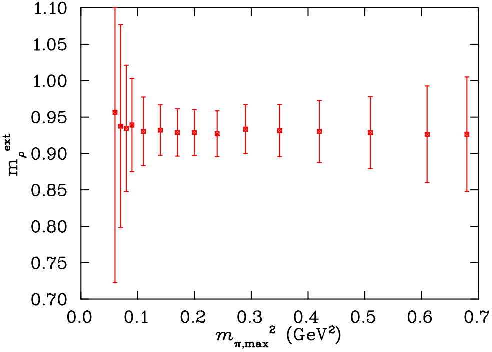

- This indicates an optimal fit window: $\hat{m}^2_{\pi,\mathrm{max}} = 0.20$ GeV^2.

Quenched ρ Meson Mass Summary

- A technique for isolating an optimal regulation scale has been tested in quenched QCD, where no experimental value of m_ρ exists to provide phenomenological bias.
- An optimal value of the maximum pion mass was also calculated. This method answers the question of how many data points we should include.
- The extrapolation correctly predicts the low-energy curvature that was observed when the low-energy lattice simulation results were revealed.
- The results clearly indicate a successful procedure for using lattice QCD results outside the PCR.

Quenched ρ Meson Mass Summary

- A technique for isolating an optimal regulation scale has been tested in quenched QCD, where no experimental value of m_ρ exists to provide phenomenological bias.
- An optimal value of the maximum pion mass was also calculated. This method answers the question of how many data points we should include.
- The extrapolation correctly predicts the low-energy curvature that was observed when the low-energy lattice simulation results were revealed.
- The results clearly indicate a successful procedure for using lattice QCD results outside the PCR.

Quenched ρ Meson Mass Summary

- A technique for isolating an optimal regulation scale has been tested in quenched QCD, where no experimental value of m_ρ exists to provide phenomenological bias.
- An optimal value of the maximum pion mass was also calculated. This method answers the question of how many data points we should include.
- The extrapolation correctly predicts the low-energy curvature that was observed when the low-energy lattice simulation results were revealed.
- The results clearly indicate a successful procedure for using lattice QCD results outside the PCR.

Quenched ρ Meson Mass Summary

- A technique for isolating an optimal regulation scale has been tested in quenched QCD, where no experimental value of m_ρ exists to provide phenomenological bias.
- An optimal value of the maximum pion mass was also calculated. This method answers the question of how many data points we should include.
- The extrapolation correctly predicts the low-energy curvature that was observed when the low-energy lattice simulation results were revealed.
- The results clearly indicate a successful procedure for using lattice QCD results outside the PCR.

Intrinsic Scale: Magnetic Moment of the Nucleon

Nucleon Magnetic Moment

- The analysis of the magnetic moment of the nucleon provides an excellent check for the identification of an intrinsic scale in the nucleon.
- Its chiral expansion similarly contains a residual series and loop integrals:

$$\mu_n = \{a_0 + a_2\, m_\pi^2\} + \mathcal{T}_N^{\mu_n}(m_\pi^2\,;\Lambda) + \mathcal{T}_\Delta^{\mu_n}(m_\pi^2\,;\Lambda) + \mathcal{O}(m_\pi^4)\,.$$

- The leading-order non-analytic term is $\chi_N^{\mu_n} m_\pi$, and we work to chiral order $\mathcal{O}(m_\pi^2)$.

Nucleon Magnetic Moment

- The analysis of the magnetic moment of the nucleon provides an excellent check for the identification of an intrinsic scale in the nucleon.
- Its chiral expansion similarly contains a residual series and loop integrals:

$$\mu_n = \{a_0 + a_2\, m_\pi^2\} + \mathcal{T}_N^{\mu_n}(m_\pi^2\,;\Lambda) + \mathcal{T}_\Delta^{\mu_n}(m_\pi^2\,;\Lambda) + \mathcal{O}(m_\pi^4)\,.$$

- The leading-order non-analytic term is $\chi_N^{\mu_n} m_\pi$, and we work to chiral order $\mathcal{O}(m_\pi^2)$.

Nucleon Magnetic Moment

- The analysis of the magnetic moment of the nucleon provides an excellent check for the identification of an intrinsic scale in the nucleon.
- Its chiral expansion similarly contains a residual series and loop integrals:

$$\mu_n = \{a_0 + a_2\, m_\pi^2\} + \mathcal{T}_N^{\mu_n}(m_\pi^2\,;\Lambda) + \mathcal{T}_\Delta^{\mu_n}(m_\pi^2\,;\Lambda) + \mathcal{O}(m_\pi^4)\,.$$

- The leading-order non-analytic term is $\chi_N^{\mu_n} m_\pi$, and we work to chiral order $\mathcal{O}(m_\pi^2)$.

Nucleon Magnetic Moment

- The analysis of the magnetic moment of the nucleon provides an excellent check for the identification of an intrinsic scale in the nucleon.
- Its chiral expansion similarly contains a residual series and loop integrals:

$$\mu_n = \{a_0 + a_2\, m_\pi^2\} + \mathcal{T}_N^{\mu_n}(m_\pi^2\,;\Lambda) + \mathcal{T}_\Delta^{\mu_n}(m_\pi^2\,;\Lambda) + \mathcal{O}(m_\pi^4)\,.$$

- The leading-order non-analytic term is $\chi_N^{\mu_n}\, m_\pi$, and we work to chiral order $\mathcal{O}(m_\pi^2)$.

Nucleon Magnetic Moment

- Consider the lattice QCD results for μ_n^{isov} from arXiv:1106.3580 [hep-lat] ($\mathcal{O}(a)$-improved Wilson quarks, $L = 1.4 \to 3.0$ fm):

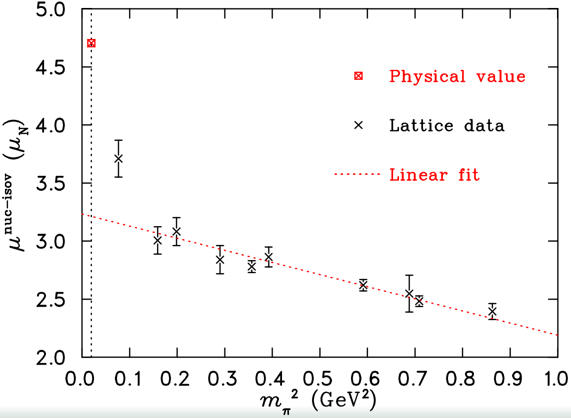

Test for an Intrinsic Scale

- The renormalization flow of c_0 is obtained using a dipole regulator:

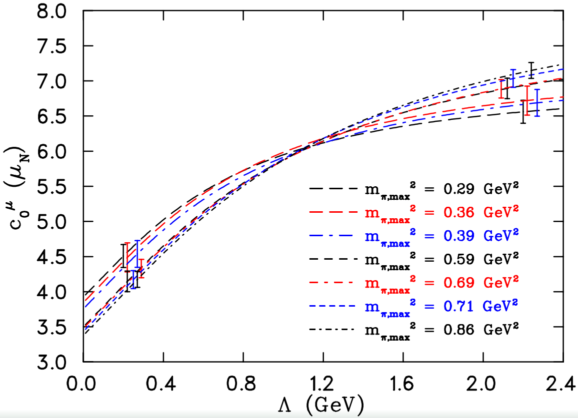

Test for an Intrinsic Scale

- The χ^2_{dof} analysis using all available results shows a distinct optimal scale of $\Lambda^{\rm scale}_{\rm dip} = 1.1$ GeV (± 0.2) GeV :

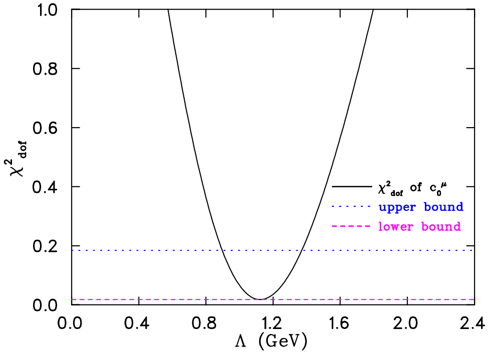

- This result is consistent with the value of $\Lambda^{\rm scale}_{\rm dip}$ obtained from the nucleon mass analysis.

Magnetic Moment: Extrapolations

- Extrapolations at finite or infinite volume, are now possible:

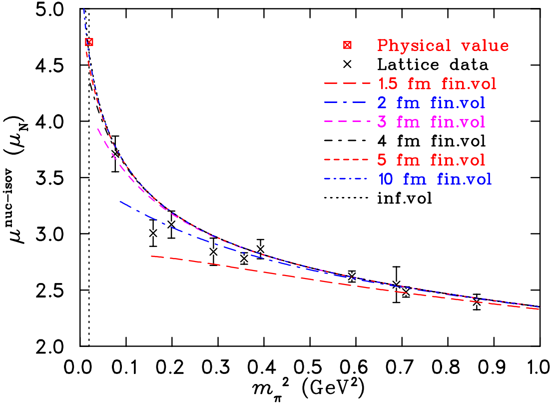

Magnetic Moment: Extrapolations

- The infinite-volume corrected data points (blue) are also shown:

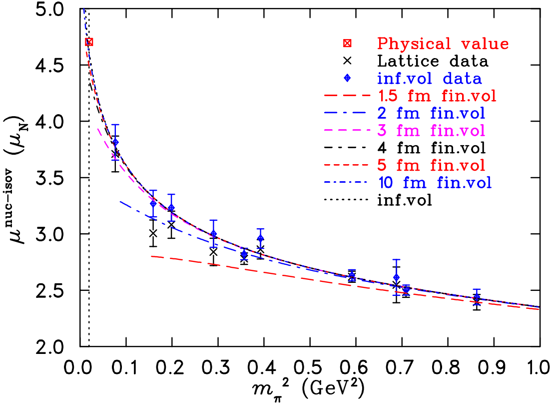

- The infinite-volume extrapolation is within 2% of the experimentally derived value $\mu_n^{\mathrm{isov}} = 4.6798\,\mu_N$.

Intrinsic Scale: Electric Charge Radius of the Nucleon

Nucleon Electric Charge Radius

- The electric charge radius (slope of the electric form form factor at $Q^2 = 0$) of the isovector nucleon affords an opportunity to explore intrinsic scales, chiral extrapolations, and subtleties in finite-volume corrections.
- Its chiral expansion similarly contains a residual series and loop integrals:

$$\langle r^2\rangle_E^{\text{isov}} = \{a_0 + a_2 m_\pi^2\} + \mathcal{T}_N^E(m_\pi^2\,;\Lambda) + \mathcal{T}_\Delta^E(m_\pi^2\,;\Lambda) + \mathcal{T}_{\text{tad}}^E(m_\pi^2\,;\Lambda) + \mathcal{O}(m_\pi^4)\,.$$

- The leading-order non-analytic term is $(\chi_N^E + \chi_t^E)\log\frac{m_\pi}{\mu}$ (where μ is a fixed mass scale), and we work to chiral order $\mathcal{O}(m_\pi^2)$.

Nucleon Electric Charge Radius

- The electric charge radius (slope of the electric form form factor at $Q^2 = 0$) of the isovector nucleon affords an opportunity to explore intrinsic scales, chiral extrapolations, and subtleties in finite-volume corrections.
- Its chiral expansion similarly contains a residual series and loop integrals:

$$\langle r^2\rangle_E^{\text{isov}} = \{a_0 + a_2 m_\pi^2\} + \mathcal{T}_N^E(m_\pi^2\,;\Lambda) + \mathcal{T}_\Delta^E(m_\pi^2\,;\Lambda) + \mathcal{T}_{\text{tad}}^E(m_\pi^2\,;\Lambda) + \mathcal{O}(m_\pi^4)\,.$$

- The leading-order non-analytic term is $(\chi_N^E + \chi_t^E)\log\frac{m_\pi}{\mu}$ (where μ is a fixed mass scale), and we work to chiral order $\mathcal{O}(m_\pi^2)$.

Nucleon Electric Charge Radius

- The electric charge radius (slope of the electric form form factor at $Q^2 = 0$) of the isovector nucleon affords an opportunity to explore intrinsic scales, chiral extrapolations, and subtleties in finite-volume corrections.
- Its chiral expansion similarly contains a residual series and loop integrals:

$$\langle r^2\rangle_E^{\rm isov} = \{a_0 + a_2 m_\pi^2\} + \mathcal{T}_N^E(m_\pi^2;\Lambda) + \mathcal{T}_\Delta^E(m_\pi^2;\Lambda) + \mathcal{T}_{\rm tad}^E(m_\pi^2;\Lambda) + \mathcal{O}(m_\pi^4)\,.$$

- The leading-order non-analytic term is $(\chi_N^E + \chi_t^E)\log\frac{m_\pi}{\mu}$ (where μ is a fixed mass scale), and we work to chiral order $\mathcal{O}(m_\pi^2)$.

Nucleon Electric Charge Radius

- The electric charge radius (slope of the electric form form factor at $Q^2 = 0$) of the isovector nucleon affords an opportunity to explore intrinsic scales, chiral extrapolations, and subtleties in finite-volume corrections.
- Its chiral expansion similarly contains a residual series and loop integrals:

$$\langle r^2 \rangle_E^{\mathrm{isov}} = \{a_0 + a_2 m_\pi^2\} + \mathcal{T}_N^E(m_\pi^2\,;\Lambda) + \mathcal{T}_\Delta^E(m_\pi^2\,;\Lambda) + \mathcal{T}_{\mathrm{tad}}^E(m_\pi^2\,;\Lambda) + \mathcal{O}(m_\pi^4)\,.$$

- The leading-order non-analytic term is $(\chi_N^E + \chi_t^E)\log\frac{m_\pi}{\mu}$ (where μ is a fixed mass scale), and we work to chiral order $\mathcal{O}(m_\pi^2)$.

Nucleon Electric Charge Radius

- Consider the lattice QCD data for $\langle r^2 \rangle_E^{\mathrm{isov}}$ from arXiv:1106.3580 [hep-lat] ($\mathcal{O}(a)$-improved Wilson quarks, $L = 1.9 \to 3.3$ fm):

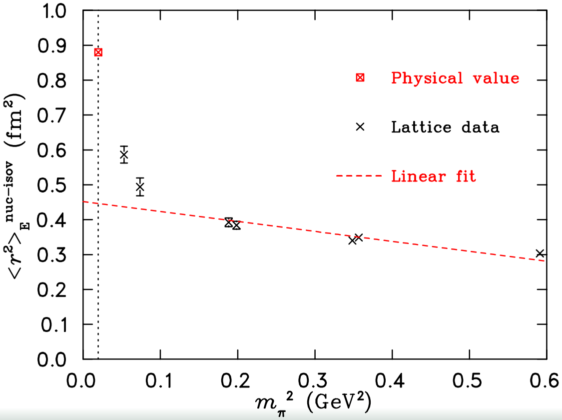

Test for an Intrinsic Scale

- The renormalization flow of $c_0^{(\mu)}$ for $\langle r^2 \rangle_E^{\mathrm{isov}}$ is obtained using a dipole regulator:

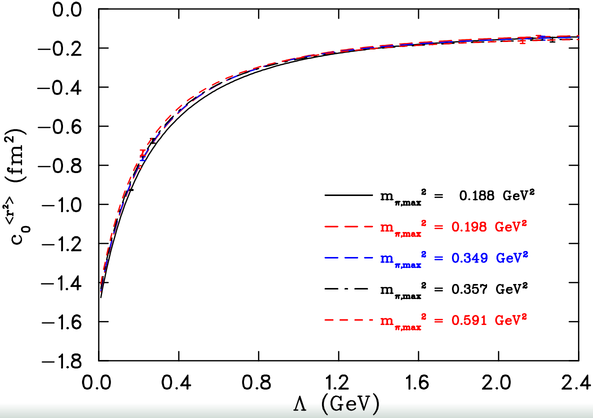

Test for an Intrinsic Scale

- The χ^2_{dof} analysis using all available data shows an optimal scale of $\Lambda^{\rm scale}_{\rm dip} = 1.67$ GeV $(+0.66 - 0.33)$ GeV :

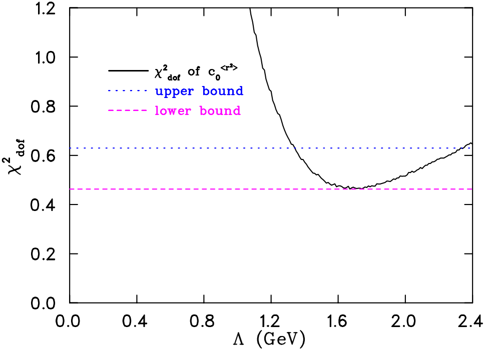

- This result is consistent with the values of $\Lambda^{\rm scale}_{\rm dip}$ obtained from the nucleon mass and magnetic moment analyses.

Electric Charge Radius: Extrapolations

- Extrapolations at finite or infinite volume, are now possible:

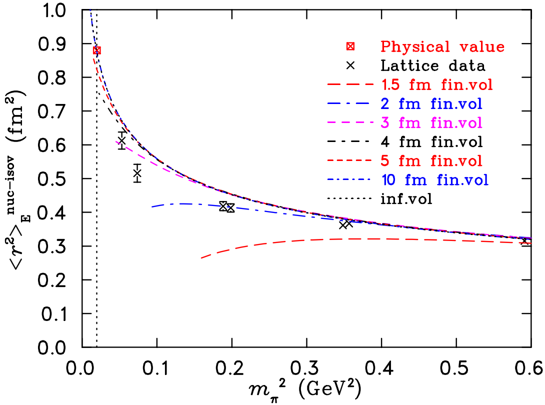

Electric Charge Radius: Extrapolations

- The infinite-volume corrected data points (blue) are also shown:

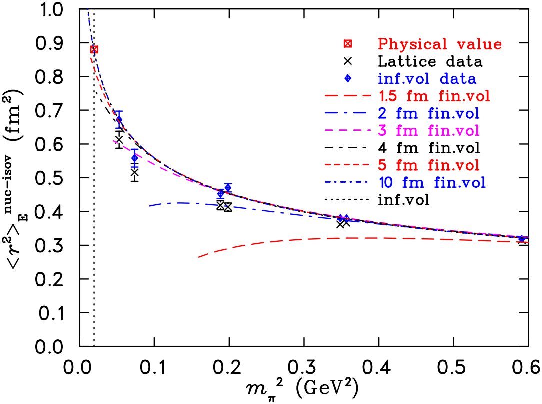

- The infinite-volume extrapolation is $\sim$ 0.5% different from the CODATA value $\langle r^2\rangle_E^{\text{isov}} = 0.88$ fm^2.

Electric Charge Radius: Extrapolations

- An estimate in the uncertainty in the extrapolation due to Λ^{scale} is marked at the physical point:

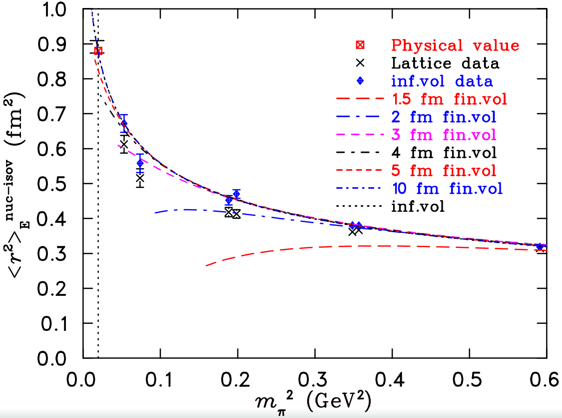

Electric Charge Radius: Extrapolations

- An estimate of the statistical uncertainty in the extrapolation is marked at the physical point:

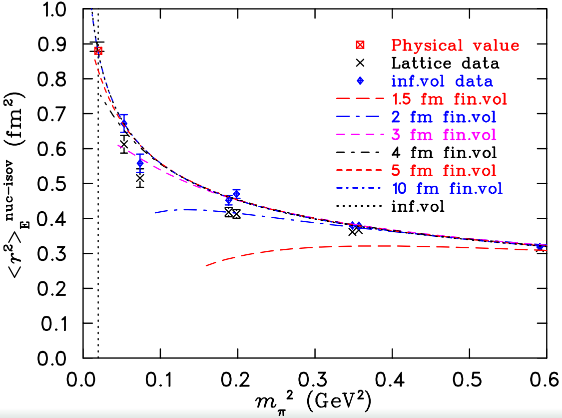

Conclusion

- The results for the intrinsic scales obtained from the nucleon mass, magnetic moment and electric charge radius are collated:

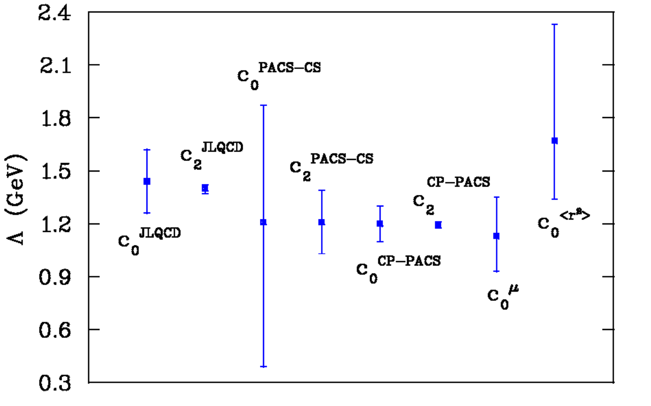

Conclusion

- We have been able to extrapolate current lattice QCD results to the physical point, using Chiral Effective Field Theory.
- We have discovered that Finite-Range Regularized Chiral Effective Field Theory is instrumental for the analysis of lattice results extending outside the chiral Power-Counting Regime.
- We have developed a robust procedure for quantifying the degree of scale-dependence, through the search for an optimal regularization scale.
- The agreement among optimal scales for the nucleon indicate the existence of an intrinsic scale, which characterizes the nucleon-pion interaction.

Conclusion

- We have been able to extrapolate current lattice QCD results to the physical point, using Chiral Effective Field Theory.
- We have discovered that Finite-Range Regularized Chiral Effective Field Theory is instrumental for the analysis of lattice results extending outside the chiral Power-Counting Regime.
- We have developed a robust procedure for quantifying the degree of scale-dependence, through the search for an optimal regularization scale.
- The agreement among optimal scales for the nucleon indicate the existence of an intrinsic scale, which characterizes the nucleon-pion interaction.

Conclusion

- We have been able to extrapolate current lattice QCD results to the physical point, using Chiral Effective Field Theory.
- We have discovered that Finite-Range Regularized Chiral Effective Field Theory is instrumental for the analysis of lattice results extending outside the chiral Power-Counting Regime.
- We have developed a robust procedure for quantifying the degree of scale-dependence, through the search for an optimal regularization scale.
- The agreement among optimal scales for the nucleon indicate the existence of an intrinsic scale, which characterizes the nucleon-pion interaction.

Conclusion

- We have been able to extrapolate current lattice QCD results to the physical point, using Chiral Effective Field Theory.
- We have discovered that Finite-Range Regularized Chiral Effective Field Theory is instrumental for the analysis of lattice results extending outside the chiral Power-Counting Regime.
- We have developed a robust procedure for quantifying the degree of scale-dependence, through the search for an optimal regularization scale.
- The agreement among optimal scales for the nucleon indicate the existence of an intrinsic scale, which characterizes the nucleon-pion interaction.

Acknowledgments

- Thank you to Derek Leinweber and Ross Young for supervision during my PhD.
- Thank you to James Zanotti, Nilmani Mathur, Keh-Fei Liu, Frank Lee and Jianbo Zhang for collaboration and support in this work.
- Thank you to Anthony Thomas, Rod Crewther and Daniel Phillips for insightful and informative discussions.

Thank You

Gary Larson (1995), *The Far Side Gallery 2*.